SKELETAL MUSCLE PURINE NUCLEOTIDE DEGRADATION AND ATROPHY: CAUSE OR CONSEQUENCE OF INCREASED URIC ACID PRODUCTION

By

Spencer Graham Miller

July, 2022

Director of Dissertation: Dr. Ron Cortright

Major Department: Kinesiology

Elevated serum uric acid is a risk factor for mortality in diseases and critical illnesses associated with skeletal muscle atrophy. Uric acid is generated by xanthine oxidoreductase (XOR) and XOR inhibitors can partially attenuate muscle atrophy. Whether purine nucleotide degradation in atrophying muscle fibers contributes to increased XOR activity and serum uric acid, and whether uric acid is sufficient to induce muscle atrophy are unknown.

Aim 1. To determine if purine nucleotide degradation is increased in atrophying skeletal muscle and its contribution to elevated uric acid production.

Muscle atrophy was induced in mice by fasting and dexamethasone (DEX), and C2C12 myotubes by DEX and constitutively active FoXO3 (caFoXO3). Purines (hypoxanthine, xanthine, uric acid) were measured in serum, extensor digitorum longus (EDL) incubation buffer, or culture media by ultra-performance liquid chromatography (UPLC). Fasting and DEX significantly increased serum uric acid and uric acid release from atrophying EDL muscles. In myotubes DEX- and caFoXO3-induced atrophy caused increased hypoxanthine and xanthine (uric acid precursors) efflux, but little to no uric acid due to lack of XOR expression. Co-culturing atrophying myotubes with endothelial cells

(which did express XOR), increased media uric acid solely from the oxidation of myotube purines. These findings demonstrate that purine nucleotide degradation coincides with increased protein degradation in atrophying skeletal muscles. Increased purine release from muscle cells can drive XOR activation in XOR-expressing cells and contributes to increased serum uric acid.

Aim 2. To determine if uric acid can directly increase muscle protein degradation and cause muscle atrophy.

C2C12 myotubes were treated with physiological levels (175, 350, or 700 μM) of uric acid for 48 hours. Myotube proteins were labeled with $^{13}C^{15}N$-Phe and changes in $^{13}C^{15}N$-Phe were quantified by UPLC and used to calculate protein degradation rates. Media and intracellular uric acid were determined by UPLC. Uric acid exposure did not increase protein degradation rates or reduce total protein in culture wells. Media uric acid was not reduced after 48 h but intracellular uric acid was significantly increased in myotubes. These findings demonstrated that while uric acid can accumulate in muscle cells, it does not directly increase muscle protein degradation or cause atrophy.

SKELETAL MUSCLE PURINE NUCLEOTIDE DEGRADATION AND ATROPHY: CAUSE OR CONSEQUENCE OF INCREASED URIC ACID PRODUCTION

A Dissertation

Presented to the Faculty of the Department of Kinesiology

East Carolina University

In Partial Fulfillment of the Requirements for the Degree

Doctor of Philosophy in Bioenergetics and Exercise Science

By

Spencer G. Miller

July, 2022

SKELETAL MUSCLE PURINE NUCLEOTIDE DEGRADATION AND ATROPHY:
CAUSE OR CONSEQUENCE OF INCREASED URIC ACID PRODUCTION

By

Spencer G. Miller

APPROVED BY:

DIRECTOR OF DISSERTATION: _____
Ronald Cortright, PhD

COMMITTEE MEMBER: _____
Jeffrey Brault, PhD

COMMITTEE MEMBER: _____
Carol Witczak, PhD

COMMITTEE MEMBER: _____
Kelsey Fisher-Wellman, PhD

COMMITTEE MEMBER: _____
Kyle Mansfield, PhD

CHAIR OF THE DEPARTMENT
OF KINESIOLOGY: _____
Joonkoo Yun, PhD

INTERIM DEAN OF THE GRADUATE SCHOOL: _____
Kathleen T Cox, PhD

ACKNOWLEDGEMENTS

I would like to thank my mentor Dr. Jeffrey Brault, without whom, none of this work would have been possible. Dr. Brault has been a wonderful mentor to me over the past seven years and I am forever grateful for his personal dedication to my growth as a scientist and professional. I would also like to thank Dr. Carol Witczak, who has also been a significant mentor to me and always willing to provide advice, resources, and a positive outlook, in times of need.

I am also very appreciative of the help and support I have received from lab-mates Paul Hafen, Cata Matias, and Andrew Law. Each of them made sacrifices and vital contributions to the successful completion of this research. They also made working the lab fun and enjoyable along the way.

Lastly, I would like to thank my fiancé Jaclyn Ruemmler and mother Amber Hutchins. Without their unrelenting love and support I would not have been able to overcome the personal and professional obstacles I've encountered during the course of this degree.

TABLE OF CONTENTS

LIST OF TABLES

LIST OF FIGURES

LIST OF ABBREVIATIONS

AMPD 1/3	AMP deaminase isoforms 1 or 3
XOR	xanthine oxidoreductase
5'NTC1A	5'nucleotidase cytosolic 1
DEX	dexamethasone
S.S.	serum starved
U.A.	uric acid
FoxO3	forkhead box class O isoform 3
caFoxO3	constitutively active FoxO3
GFP	green fluorescent protein
EDL	extensor digitorum longus
TA	tibialis anterior
3-MH	3-methylhistidine
UPLC	ultra-performance liquid chromatography

CHAPTER 1

INTRODUCTION

Skeletal Muscle Atrophy

Skeletal muscle atrophy is a debilitating condition characterized by substantial reductions in muscle size, strength, and endurance. Muscle atrophy affects a large and diverse array of clinical populations as it can occur progressively with aging and chronic diseases such as cancer, heart failure, diabetes, and renal failure [1-3], and rapidly during periods of immobilization and acute critical illness [4-7]. A major consequence of muscle atrophy is diminished muscle strength and endurance, causing patients to experience crippling weakness and fatigue that reduces their functional capacity, ability to live independently, and overall quality of life [8-10]. Most importantly, muscle atrophy greatly increases risk of mortality [11-13]. For example, 50-80% of all cancer patients will be diagnosed with cachexia (involuntary muscle wasting during disease), 80% of cancer patients diagnosed with cachexia will die within one year, and 20% of all cancer related deaths are attributed solely to cachexia [7]. In contrast, maintaining muscle mass during cancer can significantly improve chemotherapy tolerance and prolong lifespan [14, 15]. Unfortunately, despite years of dedicated research, effective pharmaceutical treatments to prevent or lessen muscle atrophy are still unavailable.

Cellular Mechanisms of Muscle Atrophy

Although pharmaceutical treatments are still unavailable, substantial progress has been made in regards to elucidating the cellular and molecular mechanisms regulating muscle atrophy during various diseases and clinical conditions [16]. At the cellular level, muscle atrophy results from heightened rates of protein degradation and/or reduced rates of protein synthesis, which combine to shift the daily balance towards net protein

degradation. Naturally, the severity and rate of muscle mass loss depends on the magnitude and duration of such imbalance.

The majority of protein degradation that occurs in skeletal muscles during atrophy is mediated by the ubiquitin-proteasome and autophagy-lysosome systems [16]. Increased activity of these pathways is enabled by the transcriptional upregulation of their protein degradation machinery (e.g., proteasome subunits and autophagosome proteins), and rate-limiting enzymes. For example, a rate-limiting step in the ubiquitin-proteasome pathway is polyubiquitination of target proteins which targets them for degradation by the 26S proteasome. This step is accomplished by a class of enzymes known as E3 ubiquitin ligases, the most well-studied of which being MuRF-1 and Atrogin-1 (also known as MAFbx1). Both of these E3 ubiquitin ligases has been found to be highly upregulated in atrophying muscles and required for its full induction during various diseases and catabolic conditions [17, 18].

Several endocrine, paracrine, and autocrine signaling mechanisms have been identified to increase muscle protein degradation gene expression during various atrophy conditions [16]. In general, these mechanisms involve modulating different intracellular signaling pathways that control the nuclear localization of transcription factors controlling the expression of protein degradation pathway genes. Some of the noteworthy transcription factors shown to be required for muscle atrophy in response to various conditions include: the forkhead box class O isoforms 1 & 3 (FoXO 1 & 3) [18], the glucocorticoid receptor (GR) [19], signal transducer and activator of transcription isoform 3 (STAT3) [20], SMAD3 [21], and nuclear factor kappa-light-chain-enhancer of activated B cells (NF-κB) [22]. Distinct intracellular signaling pathways, activated by various

extracellular factors, control the nuclear localization of these transcription factors. For example, endocrine control of FoXO 1 & 3 nuclear localization is mediated via hormones such as IGF-1 and glucocorticoids [19, 23]. IGF-1 is an anabolic hormone that inhibits FoXO nuclear localization via the IGF/PI3K/AKT signaling pathway which culminates in phosphorylation of cytosolic FoXO by AKT, which prevents its nuclear entry [23]. Conversely, the catabolic glucocorticoid hormones increase FoXO nuclear levels by binding and activating the intracellular GR, which suppresses the IGF/PI3K/AKT signaling pathway through multiple transcriptional and post-translational mechanisms [19]. Increases in glucocorticoid signaling and FoXO activation are both sufficient to induce muscle atrophy, and required for atrophy during a number of diseases, acute illnesses, and disuse conditions [24-28]. Examples of paracrine signaling mechanisms include pathways activated by proinflammatory cytokines, such as TNF-α and IL-6, which increase muscle protein degradation and atrophy through stimulation of NF-κB and STAT3 nuclear localization [20, 29]. In addition, autocrine signaling mechanisms involving pathways activated by muscle secreted myostatin, induce muscle protein degradation and atrophy via stimulation of SMAD3 nuclear localization [21].

AMPD3 upregulation and Adenine Nucleotide Depletion in Atrophying Muscle

A major discovery in the field of muscle atrophy research was the finding that there is a conserved profile of genes whose expression undergoes similar changes in atrophying muscles regardless of the upstream etiology [30]. By performing mRNA microarrays on muscles atrophying due to starvation, cancer cachexia, diabetes, and renal dysfunction, Lecker et al. identified 133 genes whose expression was similarly up or downregulated during the different atrophy conditions. A few years later, the same group expanded these findings to include spinal cord injury and muscle-specific

denervation induced atrophy [31]. As would be expected, many of the common genes were involved in the pathways of protein degradation such as the previously mentioned E3 ubiquitin ligases, MuRF-1 and atrogin-1. However, several metabolic genes belonging to pathways other than protein degradation were also identified. Despite it being almost two decades since these discoveries were made, functional roles for the altered expression of many of these genes has yet to be determined.

One of the most highly upregulated genes identified was the enzyme AMP Deaminase 3 (AMPD3). In addition to the atrophy models used in those studies, AMPD3 has been found to be among the most highly upregulated genes in muscle during aging [32], unloading [33], and Huntington's disease [34]. AMPD3 is a cytosolic enzyme that catalyzes the hydrolytic deamination of AMP to IMP and ammonia ($AMP+H_2O \rightarrow IMP+NH_3$), which is the predominant route for AMP catabolism in skeletal muscle (Fig 1.1) [35]. AMPD activity is typically low under resting conditions, but can increase rapidly upon periods of energetic stress such as intense muscle contractions and hypoxia. During these conditions, rates of ATP hydrolysis outpace rates of ATP synthesis, leading to accumulation of free ADP and AMP, and a decrease in the free energy of ATP hydrolysis ($\Delta G_{ATP}= \Delta G°_{ATP}+RTln([ADP]*[P_i]/[ATP])$) [36]. Preserving the ΔG_{ATP} requires maintaining a high

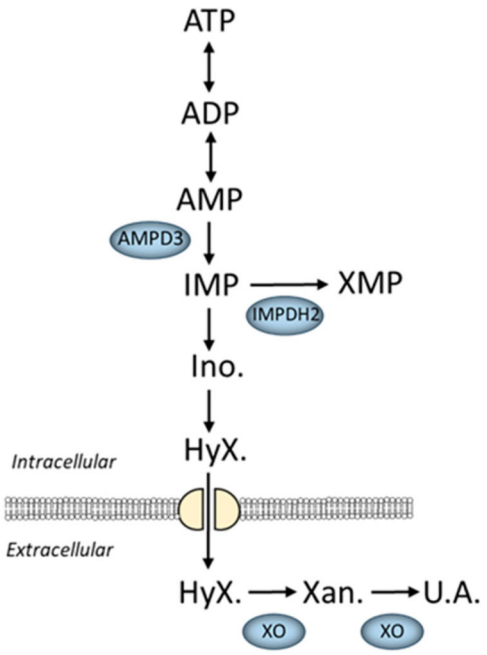

Figure 1.1. Adenine and purine nucleotide degradation pathway. Enzymes in blue are known to upregulated expression and/or activity in skeletal muscles undergoing atrophy [38].

ATP/ADP ratio, which is temporarily accomplished via the near-equilibrium adenylate kinase reaction (ADP+ADP ↔ ATP+AMP), and the thermodynamically irreversible AMPD reaction [36]. However, a major consequence of increased AMPD activity is depletion of the total adenine nucleotide pool (ATP+ADP+AMP) due to IMP flux into the purine nucleotide degradation pathway [37].

Interestingly, significant reductions in intramuscular ATP and total adenine nucleotide concentrations have been found in atrophying muscles from humans and rodents during a variety of diseases, acute critical illnesses, disuse, and aging [38]. Together, these findings would suggest that transcriptional upregulation of AMPD3, and subsequent increases in muscle fiber purine nucleotide degradation, is a fundamental mechanism of skeletal muscles atrophy. However, the cellular mechanisms controlling AMPD3 upregulation in muscles, and the downstream consequences associated with it, have not been investigated.

Purine Nucleotide Degradation

Purine nucleotide degradation involves the sequential breakdown of purine monophosphates (AMP, GMP, IMP, XMP), to purine nucleosides (adenosine, guanosine, inosine, xanthosine), and bases (adenine, guanine, hypoxanthine, xanthine). Nucleosides and bases are released from cells via concentrative and equilibrative membrane transporters, and possibly simple passive diffusion across the lipid membrane [39]. The final step of purine nucleotide degradation in humans involves the irreversible oxidation of hypoxanthine and xanthine to uric acid, catalyzed exclusively by the enzyme xanthine oxidoreductase (XOR) [40].

XOR is heterogeneously expressed in mammalian cell types, being most abundant in vascular endothelial and smooth muscle cells, intestinal epithelial cells, hepatocytes, and adipocytes [41, 42]. Its abundance is relatively low in skeletal muscle tissue homogenates, and immunohistochemical staining of healthy skeletal muscle cross sections have shown XOR to be located exclusively in the vascular endothelium [43]. As such, purine nucleosides and bases released from skeletal muscle fibers are thought to eventually undergo oxidation to uric acid in the muscle microvasculature or in peripheral XOR-expressing cell types such as hepatocytes [44].

Elevated Serum Uric Acid and Pathologies

Increases in serum uric acid are an independent risk factor for the development of numerous chronic diseases such as cancer [45], type 2 diabetes [46], kidney failure [47], heart failure [48], and cardiovascular disease [49]. It is also associated with the presence of disease risk factors such as hypertension, insulin resistance, obesity, and inflammation [50, 51]. In patients suffering various chronic diseases and acute critical illnesses, increases in serum uric acid is a strong independent predictor of mortality [45, 48, 49]. Treatment with XOR inhibitors such as febuxostat and allopurinol, has been shown to significantly decrease disease pathologies and progression [52-56], suggesting that XOR hyperactivity is directly involved in the mechanisms underlying the association between increased serum uric acid and various pathologies. Importantly, these XOR inhibitors, although used widely, do have adverse side effects, such as fatal hypersensitivity [57, 58]. Therefore, a better understanding of the role of XOR activity and uric acid production during atrophy is warranted.

XOR can produce superoxide anion as a byproduct of its reaction, which causes it be one of the major producers of reactive oxygen species in cells [40]. Numerous studies have provided evidence to support increased oxidative stress caused by XOR superoxide anion production to be the underlying mechanism linking elevated serum uric acid to cell pathologies [59]. However, direct effects of uric acid levels have also been suggested as a possible mechanism based on in vitro studies showing increased oxidative stress and inflammation in various cell types exposed to uric acid [60-64]. Moreover, other studies have provided evidence that indicates the irreversible loss of salvageable hypoxanthine and subsequent depletion of cellular purine nucleotide levels also play a role in the tissue pathologies related to elevated serum uric acid [65, 66].

Despite the seemingly universal consensus that XOR hyperactivation contributes to multiple pathologies, the upstream mechanisms and tissue sources that provide the purines which stimulate or support increased XOR activity are unknown. As mentioned previously, skeletal muscle atrophy is a prominent feature of many diseases and illnesses associated with elevated serum uric acid, and atrophying muscles are known to contain reduced concentrations of adenine nucleotides and increased expression of the adenine nucleotide degrading enzyme AMPD3. Therefore, increased release of purines from atrophying muscle may be a primary factor contributing to heightened XOR activity and serum uric acid levels.

Uric Acid and Skeletal Muscle Atrophy

XOR inhibitors have been found to partially attenuate skeletal muscle atrophy in humans and/or mice during disuse and cancer [54, 67-69]. These effects have been attributed to attenuated increases in XOR-mediated superoxide anion production, and

subsequent increases in protein oxidation and degradation. However, in a recently published study, Maarman et al. found exposing C2C12 myotubes to high levels of uric acid (750 μM) for 72 h, caused impaired mitochondrial respiration and increased the amount of oxidized lipids [70]. Moreover, exposure to high levels of uric acid has been found to increase reactive oxygen species production and oxidative stress in other cell types [60-62, 64]. Impaired mitochondrial function and oxidative stress are both indicated to cause upregulated protein degradation and skeletal muscle atrophy [71]. However, whether high levels of uric acid can directly increase muscle protein degradation and cause muscle atrophy is unknown.

Dissertation Aims

Increases in serum uric acid is an independent risk factor for disease development and mortality. These associations are known to be linked to XOR hyperactivation. However, the upstream mechanisms stimulating/supporting XOR hyperactivity are unknown. Increased purine nucleotide degradation in atrophying skeletal muscles may be an upstream event contributing to XOR hyperactivation through supply of its purine substrates. Increased XOR activity is also implicated to stimulate increases in skeletal muscle protein degradation and muscle atrophy. However, whether this effect is directly caused by increased levels of uric acid is unknown. Therefore, this dissertation sought to address the following aims:

Aim 1. To determine if purine nucleotide degradation is increased in atrophying skeletal muscle and its contribution to elevated uric acid production.

Aim 2. To determine if uric acid can directly increase muscle protein degradation and cause muscle atrophy.

CHAPTER 2

Xanthine oxidoreductase activity and uric acid formation are driven by purine release from atrophying muscle

ABSTRACT

Background: Increased serum uric acid (SUA), the end product of purine nucleotide degradation in humans, is an independent risk factor for disease and mortality. Skeletal muscle atrophy and weakness are prevalent in diseases associated with increased SUA, and atrophic muscles have upregulated expression of AMP deaminase 3 (AMPD3, AMP→IMP+NH_3), a rate-limiting enzyme in adenine nucleotide degradation. However, whether purine nucleotide degradation is increased in atrophying myofibers, and whether myofiber purine release drives uric acid synthesis, are unknown.

Methods: SUA and 3-methylhistidine/1-methylhistidine (3-MH/1-MH) were measured in women matched for lean mass but with average or low physical performance (n=20/group). To induce muscle atrophy, C57BL/6J mice were fasted (48h) or injected with dexamethasone (DEX; 5 days). C2C12 myotubes were treated with DEX or constitutively active FoxO3 (caFoxO3). Purines (hypoxanthine, xanthine, UA) were measured in serum, EDL incubation buffer, or culture media by UPLC. AMPD3 promotor activity was determined by custom luciferase reporter and protein expression by western blot. Myotube purines were labeled by media $^{13}C^{15}N$-glycine, then co-cultured with bovine aortic endothelial cells (BAOEC) during DEX. Media $^{13}C^{15}N$-UA was measured by UPLC-MS.

Results: Low performers had higher SUA (3.5±1.0 vs. 2.8±0.4 mg/dL) and a trend for higher 3-MH/1-MH (p=0.06). In mice, SUA was increased 38% by fasting, and 17% by DEX. EDL UA release was increased 33% by fasting, and 30% by DEX. DEX treated

myotubes had 1.9- and 2.2-fold greater hypoxanthine and xanthine release, a 4-fold increase in AMPD3 protein expression, and a 1.6-fold increase in AMPD3 promotor activity. caFoxO3 expressing myotubes had 9.2- and 5.9-fold greater hypoxanthine and xanthine release, a 3.5-fold increase in AMPD3 protein expression, and a 3.8-fold increased AMPD3 promotor activity. The increase in AMPD3 promotor activity during DEX and caFoxO3 treatments was completely attenuated by mutating the FoxO binding sites in the AMPD3 promotor region. Compared to hypoxanthine and xanthine, myotube UA release was minimal, and protein expression of xanthine oxidoreductase (XOR), which oxidizes hypoxanthine/xanthine to UA, was undetectable. Co-culturing myotubes with BAOEC, which did express XOR, caused 3.7-fold increased UA, all of which originated from the myotubes.

Conclusions: Fasting, glucocorticoids, and FoxO, increase AMPD3 expression, purine nucleotide degradation, and purine efflux from skeletal muscle. Muscle purine release drives XOR activation and UA synthesis by XOR-expressing cell types and contributes to increased SUA. Preventing muscle purine nucleotide degradation could be a novel strategy for treating pathologies associated with increased XOR activity and SUA.

INTRODUCTION

Increases in serum uric acid is an independent risk factor for the development and poor prognosis of many pathologies including cancer [45], cardiovascular disease [48, 49], pulmonary disease [72], chronic kidney disease [47, 73], type 2 diabetes [46], and liver disease [74]. It is also positively associated with disease risk factors such as the components of metabolic syndrome [50], and a heightened inflammatory state [51]. Uric acid is produced exclusively by the enzyme xanthine oxidoreductase (XOR), which catalyzes the irreversible oxidation of hypoxanthine and xanthine in the final step of purine nucleotide degradation in humans. Despite the abundance of clinical and pre-clinical evidence linking elevated XOR activity and uric acid production to the aforementioned pathologies, the upstream processes responsible for an increase in serum uric acid are poorly understood.

XOR is heterogeneously expressed in mammalian cells and tissues, being most abundant in vascular endothelial cells, intestinal epithelial cells, hepatocytes, and adipocytes [41-43] Its substrates, hypoxanthine and xanthine, are produced from the breakdown of purine monophosphates (AMP, GMP, IMP, and XMP), which are generated from the catabolism of ATP/GTP, DNA/RNA, or de novo purine nucleotide synthesis. In cell types that do not express XOR, such as skeletal muscle fibers [75], purine nucleotide degradation is presumed to culminate in the release of hypoxanthine and xanthine, which eventually undergo oxidation in a XOR-expressing cell type or by circulating XOR [37, 44]. Thus, because XOR-expressing cells can oxidize their own purines and those generated in non-XOR expressing cells, and because XOR is expressed in vascular endothelial cells which reside in all tissues, the predominant cellular source(s) supplying

purine precursors for uric acid formation are unknown. Identifying the sources will provide valuable mechanistic insights into the link between increased serum uric acid and diseases, and possibly lead to novel targets for preventing or treating numerous pathologies.

Several lines of evidence implicate skeletal muscle fibers as being a major source of purine precursors used for increased uric acid formation. Skeletal muscles are the most abundant bodily tissue, contain the greatest concentrations of purine nucleotides [76], and have enzymatic capacity for de novo purine synthesis [77]. Skeletal muscle atrophy is a common feature of diseases and conditions associated with increased serum uric acid, and widely reported to involve significant reductions in intramuscular ATP and total adenine nucleotide concentrations [38]. Rodent studies have identified AMP deaminase 3 (AMPD3) as one of the most highly upregulated genes in muscles atrophying in response to diseases [30], disuse/unloading [78, 79], and aging [32, 80]. AMPD catalyzes the rate-limiting step in adenine nucleotide degradation ($AMP \rightarrow IMP + NH_3$), and we have previously shown its overexpression in muscle is sufficient to increase purine nucleotide degradation [81, 82]. However, whether purine nucleotide degradation is increased in skeletal muscles during atrophy, and the potential for increased muscle purine release to causes substrate driven activation of XOR and uric acid formation are unknown.

Therefore, the goals of this study were to determine if purine nucleotide degradation is increased in atrophying skeletal muscle, and, if so, to determine the contribution of increased muscle purine efflux to uric acid production. To address these goals, we utilized targeted UPLC-MS methods to compare serum uric acid and markers of protein degradation in humans, analyzed serum uric acid and purine release from

mouse muscles during fasting- and glucocorticoid-induced atrophy, and performed in vitro co-culture experiments to dissect the cellular mechanisms controlling muscle purine nucleotide degradation and its contribution to increased uric acid production.

METHODS

Human subjects

De-identified physical function assessment records and non-fasted blood samples were procured through the Musculoskeletal Function, Imaging, and Tissue Resource Core (FIT Core) at the Indiana Center for Musculoskeletal Health (ICMH). The participants' data were classified according to physical performance into Low or Average groups using normative data collected by the FIT Core [83]. Forty records, all female, were selected to meet the quotas for each performance group yet matched for age, height, weight, and body mass index. Patients <18 years old, > 80 years old, with a known history of chronic kidney disease, gout, or those who were taking uric acid-lowering medications (e.g. allopurinol, febuxostat) were excluded. Two subjects did not undergo a Dual Energy x-Ray Absorptiometry (DEXA) scan and were excluded from the analysis of appendicular lean mass / height^2.

Animals

C57BL/6J mice (13-15 wk) were acquired from Jackson Laboratories and then housed in groups of 2-5 per cage with free access to food and water. For fasting studies, animals were placed in a clean cage starting at 10:00 AM with normal access to water and food, or water only, for 48 h. For dexamethasone studies, animals were subcutaneously injected once daily for 5 days with 5 mg/kg body weight veterinary grade dexamethasone

(Dexium, Bimeda) or vehicle. Prior to beginning our investigations, we obtained approval from the Indiana University School of Medicine (IUSM) Institutional Animal Care and Use Committee (IACUC protocol #19149).

Ex vivo skeletal muscle incubations

Mice were anesthetized by I.P. injection of ketamine (90mg/kg)/xylazine (10mg/kg) and kept on a 37°C heating pad, breathing 100% O_2 throughout muscle collection. Proximal and distal tendons of the EDL muscle were carefully tied with silk suture, and muscles were quickly excised, weighed, and vertically hung in a 2 mL bath of Krebs-Henseleit buffer (25 mM $NaHCO_3$, 118 mM NaCl, 4.7 mM KCl, 1.2 mM $MgSO_4$, 1.2 mM KH_2PO_4, 1.2 mM $CaCl_2$, 5mM glucose, 0.15 mM sodium pyruvate) being continuously gassed with 95% O_2/5% CO_2 at 37°C. After 30 min pre-incubation, muscles were moved to a fresh 2 mL bath, and aliquots of buffer were collected 1h and 2h later. Buffer samples were kept on ice and then frozen at -80°C. After 2hrs, muscles were blotted and frozen in liquid nitrogen.

Cell Culture

C2C12 mouse myoblasts (ATCC) were grown on gelatin-coated (Sigma G9391) 6-well plates in Dulbecco's modified Eagle's medium (DMEM) containing 4.5 g/L glucose, L-glutamine, and sodium pyruvate, and supplemented with 10% heat inactivated fetal bovine serum (Gibco 16140-071), and penicillin (100 IU/mL)/streptomycin (100 µg/mL). When myoblasts were 75-90% confluent, media was switched to DMEM with 2% horse serum (Hyclone SH30074.03) and penicillin/streptomycin to induce differentiation into multi-nucleated myotubes. Bovine Aortic Endothelial Cells (Sigma B304-05) were grown

on 6-well plates in BAOEC growth medium (Cell Applications). AML-12 hepatocytes (ATCC CRL-2254) were grown on 6-well plates in DMEM-F12 medium supplemented with 10% FBS, penicillin/streptomycin, 10 µg/ml insulin, 5.5 µg/ml transferrin, 5 ng/ml selenium, and 40 ng/ml dexamethasone. 3T3-L1 mouse embryonic fibroblasts (ATCC CL-173) were grown in 6-well plates in “pre-adipocyte” medium (DMEM supplemented with 10% FBS and penicillin/streptomycin) which was refreshed every 48 h. After reaching 100% confluency, cells were maintained in pre-adipocyte medium for another 48 h and then switched to “differentiation medium” (DMEM supplemented with 10% FBS, Pen/Strep, 1 µM dexamethasone, 0.5 mM methylisobutylxanthine, and 1 µg/mL insulin). Cells were incubated in differentiation medium for 48 h and then switched to “adipocyte maintenance” medium (DMEM supplemented with 10% FBS, Pen/Strep, 1 µg/mL insulin). Cells were maintained in adipocyte maintenance medium for 14 days with media being refreshed every 48 h. C2C12, BAOEC, and AML-12 cells were maintained at 37°C and 5% CO_2, and 3T3-L1 were maintained at 37°C and 8% CO_2. Dexamethasone (MP Biomedicals cat. 190040) was dissolved in DMSO to a stock concentration of 100 mM (1000x greater than highest experimental concentration). The stock solution was then diluted in culture media, and DMSO volumes equal to those used in the highest experimental concentration were given as a control. For exogenous purine treatment, hypoxanthine (Sigma #H9377), xanthine (Sigma #X0626), and allopurinol (Sigma #A8003) were dissolved in 1M NaOH. Stock solutions were then diluted in the appropriate media for each cell type.

Purine quantification

Media samples were thawed at room temperature, placed on ice, and then diluted 1:4 with cold (-20°C) 80% methanol to precipitate proteins. Samples were incubated at -20°C for 20 minutes, followed by centrifugation for 10 min at 20,000xg at 4°C. An aliquot of the supernatant was lyophilized using a Vacufuge plus (Cat 5305, Eppendorf, Enfield, CT, USA) and resuspended in miliQ H_2O before UPLC analysis with Waters Acquity UPLC H-Class Bio system with UV absorbance, as we have done previously [84]. Samples were separated with an Acquity Premier HSS T3 column with 1.8 µm VanGuard fit 2.1 X 150 mm (p/n 186009472, Waters, Milford, MA, USA) at 40°C and a 0.4 mL/min flow rate. Mobile phase A (pH 4.95) contained 10 mM ammonium acetate and 1 ppm citric acid. Mobile phase B (pH 4.95) consisted of 10 mM ammonium acetate, 1 ppm citric acid, 75% acetonitrile (34998, HPLC Plus, MilliporeSigma), and 5% methanol (HPLC Grade A452, FisherScientific). Quantification of purines was done by comparing peak area at 290nm for uric acid, or 254nm for other purines, to known amounts of injected pure compounds.

Amino acid quantification

Amino acid levels were measured using derivatization of amine groups using the AccQ-Tag Ultra kit (SKU 186003836, Waters, Milford, MA, USA). Briefly, proteins were precipitated with methanol, and the supernatant was lyophilized using a Vacufuge plus. Samples were reconstituted in molecular-grade water (46-000, Corning, NY, USA) at a volume three times the original sample. The derivatization was performed as directed by manufacturer instructions with 70 µL of borate buffer plus 15 µL of sample plus 15 µL AccQ-Tag Ultra reagent combined in a glass screw neck vial (p/n 186000384c, Waters). The samples were analyzed with an AccQ-Tag Ultra C18 1.7µm column (p/n 186003837, Waters) on a Waters Acquity UPLC system and quantified by absorbance at 260 nm.

Protein Degradation rates

Protein degradation assay is based on our previous work using a radiolabeled amino acid to label the protein pool [81, 85-87]. In the current study, we have adapted this protocol to use stable isotope labeling. C2C12 myoblasts were allowed to differentiate in DMEM supplemented with 2% HS, 1% PenStrep, and $^{13}C_9{}^{15}N$-phenylalanine (130 mg/L, Sigma #608017). Four days later, myotubes were washed twice with normal unlabeled DMEM, with additional washes repeated 1 and 2 h later to allow degradation of short-lived proteins. After the second chase period, atrophy treatments were initiated and media samples were collected over time for measurement of $^{13}C_9{}^{15}N$-phenylalanine by UPLC and mass detection (Waters Acquity UPLC system with Acquity QDa mass detector).

AMPD3 promoter luciferase reporter assay

The 1.1 kb genomic promoter sequence ranging from 1000 bases 5' to 100 bases 3' of the mouse AMPD3 transcriptional start site (TSS) was synthesized by Genscript and inserted in the XhoI/HindIII cloning site of the pNL1.1[Nluc] reporter plasmid (Promega). A consensus FoxO binding site, GTAAACAACTG, is located at 124 bases upstream of the TSS. To inactivate this site, Q5 Site-directed Mutagenesis Kit (New England Biolabs) was used to mutate this sequence to GTCCACAACTG. This is termed the ΔFoxO mutant. The full sequences of the wild-type promoter and the ΔFoxO promoter were confirmed by Sanger sequencing (Azenta Life Sciences). Myoblasts were transfected 24 h prior to differentiation. Nano-Glo luciferase activity reporter assays (Promega, N1630) were conducted according to manufacturer's protocol. Briefly, myotubes were harvested in passive lysis buffer supplied in the assay kit and luciferase activity was measured by plate

reader. An aliquot of lysate was used to quantify protein concentration by BCA assay. Raw luminescence values were normalized to total protein.

Co-culture experiments

C2C12 myoblasts and myotubes were grown on gelatin coated 6-well plates (Corning) in DMEM supplemented with $^{13}C_2{}^{15}N$-Glycine (30 mg/L, Cambridge Isotope Laboratories CAS#211057-02-2) in order to uniformly label the intracellular purine nucleotide pool. BAOEC cells were grown on 6-well cell culture inserts (0.4 μM transparent membrane, ThinCerts, Greiner Bio-One). At the start of treatments, BAOEC cultures were inserted into the C2C12 myotube containing well. Media samples were collected and analyzed for hypoxanthine, xanthine, and uric acid by UPLC/MS.

Western Blotting

Proteins were extracted from cells in radio-immunoprecipitation (RIPA) buffer including protease and phosphatase inhibitors (Roche) and quantified by BCA Assay (Pierce). Proteins (10-15 μg) were separated by SDS-PAGE (7.5-12% BioRad TGX stain-free gels) then transferred to polyvinylidene difluoride (PVDF) membranes. Equal protein loading and transfer of was confirmed by capturing protein fluorescence after photoactivation of gels and transfer to membranes. Membranes were blocked for 1 h at room temperature using a 5% bovine serum albumin (BSA, Sigma A7906) dissolved in Tris buffered saline with 0.1% tween 20 (TBS-T) solution. Primary antibodies were purchased from Invitrogen (AMPD3 PA5-76912, 5'NT1CA PA5-101545), Abcam (XOR ab109235), Santa Cruz (AMPD1 D-7) and diluted 1:1000 in TBS-T plus 5% BSA. Membranes were incubated in primary antibody overnight at 4°C with rocking. Secondary

antibodies conjugated to horseradish peroxidase (Cell Signaling #7074, ThermoFisher #31444) were diluted 1:5000 in TBS-T plus 2% BSA and membranes were incubated at room temperature for 1 h. Proteins were detected with Western Chemiluminescence HRP Substrate (EMD Millipore). Band intensities were captured using a Bio-Rad Chemi Doc XRS imager and analyzed using Image Lab Software 6.1 (Bio-Rad). Approximate molecular weights of protein were calculated relative to PageRuler Plus protein ladder (ThermoFisher).

MyHC/DAPI staining, imaging, quantification

Myotube area was determined by quantifying the total area of myosin heavy chain per well as we have done previously [86]. Myosin heavy chain was detected by immunofluorescent staining of myosin heavy chain (primary antibody: #A4.1025; DSHB U. Iowa; secondary antibody: Alexafluor 546 goat anti-mouse IgG #A11030 Life Technologies) and nuclei were stained using DAPI. MyHC area was calculated by quantifying the area of red fluorescent pixels per image using ImageJ software.

Statistics

Unless stated otherwise, all data are presented as mean ± standard deviation. Statistical analyses were performed using GraphPad Prism 9. Data were tested for normality using Shapiro-Wilk normality test and Spearman's test for heteroscedasticity. Data with unequal variance were log transformed prior to analysis. All cell culture experiments were repeated at least twice in order to confirm reproducibility.

RESULTS

Serum uric acid is greater in individuals with low physical performance

Reductions in muscle function and functional capacity often proceed loss of muscle mass [88, 89]. To determine whether uric acid is increased in humans with poor physical performance, we compared serum uric acid levels in women that scored average or below average on multiple standard clinical physical performance tests (N=20/group). Subjects were matched for age, height, weight, body mass index (BMI), and estimated lean body mass (appendicular mass/height^2) (Table 2.1). Low performers had lower max grip strength, longer time to complete 5 sit-to-stands, fewer sit-to-stands completed in 30 s, and a trend (p=0.06) for shorter 6 min walking distance (Table 2.1). Serum uric acid levels were significantly greater in low vs. average physical performance groups (3.59 ± 1.04 vs. 2.86 ± 0.49 mg/dL) (Fig. 2,1A), while no differences in serum creatinine or creatine kinase (markers of kidney function, muscle mass, and muscle damage) were detected (Table 2.1). Serum levels of 3-methylhistidine (3-MH), an amino acid found predominantly in myofibrillar actin and myosin [90], is a marker of endogenous muscle protein degradation. However, serum 3-MH is also influenced by dietary meat intake[90] . Therefore, the serum ratio of 3-MH to 1-MH (which is uniquely found in animal muscle [90]), can be used to account for the influence of dietary protein and more accurately estimate endogenous muscle protein turnover during non-fasted states [91]. No differences in 3-MH were detected between groups (Fig. 2.1B). However, serum 1-MH trended higher in average performance groups (p=0.06, Fig. 2.1C), and serum 3-MH/1-MH trended higher in low performance groups (p=0.06, Fig. 2.1D). Collectively, these findings suggested a possible relationship between serum uric acid and increased skeletal muscle protein degradation.

Efflux of uric acid is increased in skeletal muscles after fasting and dexamethasone treatment

To determine if atrophying skeletal muscles have increased purine nucleotide degradation, we measured release of purine nucleotide degradation products (hypoxanthine, xanthine, uric acid) from ex vivo incubated EDL muscles after 48 h of fasting. Fasting caused a reduction in body and EDL weight (Fig. 2.2A & B), and a 38% increase in serum uric acid (Fig. 2.2C). EDL muscles from fasted mice released similar amounts of hypoxanthine and xanthine (Fig. 2.2D & E) but 33% more uric acid than non-fasted controls (Fig. 2.2F). However, no differences in protein expression of the adenine nucleotide degrading enzymes AMPD 1 & 3, cytosolic 5'nucleotidase 1 (5'NTC1a), or XOR were detected in the EDLs (Fig. 2.2G-J). Though, we did detect an increase in AMPD3 protein levels in fasted tibialis anterior muscles (Fig. 2.2L). Unfortunately, we are unable to measure purine release from TA muscles because they are too large to allow sufficient oxygen perfusion during ex vivo incubations [92], hence any differences in purine efflux would be confounded by hypoxia.

Increased muscle protein degradation in response to fasting, sepsis, and many chronic diseases states, is partly mediated by increased circulating glucocorticoids [19]. To determine if increased glucocorticoid exposure is sufficient to increase muscle purine efflux, mice were injected with the synthetic glucocorticoid dexamethasone (DEX) for 5 days and purine efflux was measured from isolated EDL muscles. DEX treatment did not cause a significant reduction in EDL weights (Fig. 2.3A & B) but did cause a 17% increase ($p=0.05$) in serum uric acid (Fig. 2.3C). Additionally, EDL muscles from DEX treated mice had increased rates of myofibrillar protein degradation as evidenced by 37% greater 3-

MH release (Fig. 2.3D), suggesting that atrophy was occurring. EDL muscles from DEX treated mice released similar amounts of hypoxanthine and xanthine (Fig. 2.3E & F), but 27% more uric acid, compared to vehicle treated controls (Fig. 2.3G). Moreover, a positive correlation was found between EDL uric acid and 3-MH release (r^2= 0.34; p=0.013; Fig. 2.3H). No differences in protein expression of purine nucleotide degrading enzymes were detected in DEX treated EDL muscles (Fig. 2.3I-L). However, similar to fasted mice, an increase AMPD3 protein was observed in DEX treated TA muscles (Fig. 2.3N).

Purine nucleotide degradation and purine efflux are increased in atrophying muscle cells

In addition to muscle fibers, muscle tissue is comprised of numerous other cell types such as vascular endothelial cells, macrophages, fibro-adipogenic progenitor cells, and satellite cells [93]. Moreover, immunohistochemical staining of skeletal muscle cross-sections have shown XOR expression localized to vascular cells and possibly macrophages [75]. To determine if purine nucleotide degradation is specifically upregulated in muscle cells during atrophy, purine release was measured from C2C12 myotubes during DEX and/or serum starvation (S.S.) treatments. After 48 h, myotube atrophy was confirmed by quantifying myosin heavy chain (MyHC) area (Fig. 2.4A). Myotubes treated with 10 or 100 μM DEX had less MyHC area (Fig. 2.4B), but no differences in nuclei count, compared to vehicle (Fig. 2.4C). S.S. myotubes had the lowest MyHC area, but also contained less nuclei (Fig. 2.4C). The reductions in MyHC area were preceded by increases in protein degradation rates between 6 and 24 h post-DEX and/or S.S. treatment (Fig. 2.4D-G).

After validating that these treatments cause atrophy, we determined if purine nucleotide degradation was increased by measuring hypoxanthine, xanthine, and uric

acid in the media over time. DEX caused a significant increase in hypoxanthine (Fig 2.4H) and xanthine (Fig. 2.4I) release by 12h, eventually reaching peak levels at 48h that were 3.6- and 1.8-fold greater than vehicle, respectively. The increase was similar among the different DEX doses tested (Sup. Fig. 2.1). S.S.+Veh also caused an increase in hypoxanthine release, which peaked by 24 h and then remained unchanged (Fig. 2.4H). Combining S.S.+DEX resulted in the greatest hypoxanthine release among groups, and similar to S.S.+Veh, remained unchanged after peaking by 24 h (Fig. 2.4H). Interestingly, S.S. negatively affected xanthine release, with S.S.+Veh groups releasing less xanthine than Veh treated, and S.S.+DEX groups releasing more than S.S.+Veh and Veh, but less than DEX (Fig. 2.4J). Importantly, unlike its precursors hypoxanthine and xanthine, uric acid was undetected in all groups until 36 h, when it was detected in DEX groups at a miniscule 0.4 nmoles/well (Fig. 2.4J). By 48 h it had risen to 2 nmoles/well in DEX, and 0.5 nmoles/well in S.S.+DEX groups, respectively (Fig. 2.4J). These increases in purine efflux in response to DEX coincided with a 4-fold increase in AMPD3 protein expression (Fig. 2.4L & N), whereas XOR was virtually undetectable except for a faint, but unquantifiable, band in SS+DEX groups (Fig. 2.4M).

Increased FoxO3 activity is sufficient to increase purine nucleotide degradation and AMPD3 protein expression in myotubes

Glucocorticoids and fasting induce muscle atrophy, in part, by increasing the activity of FoxO transcription factors [18, 23, 24]. Therefore, to determine if increased FoxO activity is sufficient to stimulate muscle purine nucleotide degradation, we transduced C2C12 myotubes with adenovirus encoding a constitutively active FoxO3 isoform (caFoxO3) [25] and measured the effect on purine efflux. As expected [18],

caFoxO3 expression dramatically reduced MyHC area compared to GFP expressing controls (Fig. 2.5B), but not total nuclei count (Fig. 2.5C). Moreover, caFoxO3 caused an increase in media hypoxanthine (Fig 2.5D) and xanthine (Fig. 2.5E), while uric acid was undetected (Fig. 2.5F), demonstrating that increased FoxO activity is sufficient to increase purine nucleotide degradation in muscle. As with DEX treatment, the elevated production of hypoxanthine and xanthine was accompanied by demonstrable upregulation of AMPD3 (Fig. 2.5G). The AMPD3 promotor region contains a consensus FoxO binding 124 bases upstream of the transcriptional start site. Therefore, to determine if the increases in AMPD3 protein were related to FoxO-dependent activation of its promotor region, we transfected myoblasts with custom luciferase reporter plasmids containing 1.1 Kb of the wildtype AMPD3 proximal promotor region, with or without a substitution mutation in the FoxO binding site (ΔFoxO mutant). Increased FoxO expression was sufficient to increase AMPD3 promotor activity, which was prevented by mutating its binding site in the AMPD3 promotor region (Fig. 2.5H). Moreover, AMPD3 promotor activity was also increased by DEX and S.S. treatment by FoxO dependent mechanism (Fig. 2.5I).

Purines released from atrophying myotubes drive uric acid formation by XOR-expressing cells

After finding that myotube atrophy involved increased efflux of hypoxanthine and xanthine, with only marginal XOR expression and uric acid production, we sought to determine if myotube purines could be oxidized to uric acid by XOR expressing cell types. XOR expression is strongly detected in liver, lung, small intestine, heart, aorta, and adipose tissue homogenates [41]. In immortalized cell lines, its expression is reported in bovine aortic endothelial cells (BAOEC) [94], 3T3-L1 adipocytes [41], and AML-12

hepatocytes [41]. We confirmed XOR protein expression in these cell types (Fig. 2.6A) and tested whether they could oxidize exogenous purines by measuring media changes in uric acid after exposing them to physiological levels of hypoxanthine and xanthine. All four cell types (C2C12, BAOEC, 3T3-L1, AML-12) consumed exogenous hypoxanthine as demonstrated by progressive reductions in its media concentrations (Sup. Fig. 2.2). However, only XOR expressing cells consumed xanthine (Sup. Fig. 2.2). In cell types expressing XOR, hypoxanthine and xanthine both caused dramatic increases in uric acid production, which was completely attenuated by the XOR inhibitor allopurinol (Fig. 2.6B, Sup. Fig. 2.2). We then tested whether co-culturing myotubes with BAOEC would enable the oxidation of purines released from myotubes, and whether myotube atrophy would stimulate an increase in uric acid formation. Prior to the co-culture period, myotube purines were labeled using $^{13}C^{15}N$-glycine, which supplies two carbons and a nitrogen atom to the purine ring during de novo purine synthesis (Fig 2.6D). At the start the co-culture, $^{13}C^{15}N$-glycine medium was replaced with normal medium containing vehicle or DEX, and added to wells containing C2C12 only, BAEOC only, or C2C12+BAOEC. As before, DEX significantly increased hypoxanthine, xanthine, and uric acid release (Fig. 2.6C). However, media uric acid was 3.5- and 9.5-fold greater in C2C12+BAOEC co-cultures vs. C2C12 or BAOEC (Fig 2.6C). In addition, heavy labeled uric acid (with a weight of 170 Da) was only detected in wells containing myotubes, and was 2.8-fold greater in C2C12+BAOEC vs. C2C12 after DEX (Fig 2.6E). Interestingly, despite the substantial increase in uric acid production in C2C12+BAOEC co-cultures, the percentage of heavy labeled uric acid per total uric acid was similar between C2C12 and

C2C12+BAOEC after DEX (Fig 2.6F), indicating that uric acid was derived solely from myotube purines.

DISCUSSION

The present study sought to determine if purine nucleotide degradation and purine release are increased in skeletal muscles undergoing atrophy, and whether elevated muscle purine release could stimulate increased uric acid synthesis. In humans, serum uric acid was greater in individuals with below average physical performance, suggesting it may be an early indicator of muscle atrophy. In mice, fasting- and glucocorticoid-induced atrophy, coincided with increased serum uric acid and uric acid efflux from EDL muscles. In cultured myotubes, glucocorticoid- and constitutively active FoxO3-induced atrophy coincided with increased hypoxanthine and xanthine efflux but little to no uric acid production, which is consistent with the lack of XOR. Co-culturing myotubes with XOR-expressing aortic endothelial cells, which do express XOR, enabled the oxidation of myotube released hypoxanthine and xanthine to uric acid. Thus, our findings demonstrate that purine nucleotide degradation and purine release are increased in muscle cells undergoing atrophy in response to fasting, glucocorticoids, and increased FoxO3 activity. Increased muscle purine release stimulates uric acid formation by adjacent XOR-expressing cells.

Reductions in contractile function and increases in protein degradation often proceed loss of skeletal muscle mass and sarcopenia [30, 88, 89]. We found that women with below average physical performance, but equal levels of lean body mass, had higher serum uric acid and a trend for increased serum 3-MH/1-MH, suggesting that these subjects may be pre-sarcopenic. These findings indicate that serum UA levels could be

a sensitive biomarker for increased muscle protein degradation, a notion supported by our animal data showing a positive correlation between EDL 3-MH and UA release. This could be of clinical use for predicting risk of muscle atrophy. Longitudinal studies comparing serum uric acid, muscle mass, and muscle protein degradation rates during atrophic and non-atrophic conditions would further elucidate the utility of uric acid as a diagnostic biomarker for sarcopenia.

Our use of an ex vivo incubation approach demonstrates that purine nucleotide degradation is increased specifically in whole muscle tissue during atrophy by fasting or dexamethasone. This is consistent with studies demonstrating increases in hypoxanthine, xanthine, and/or uric acid concentration in muscle homogenates during other atrophy conditions such as mechanical ventilation [68], type 2 diabetes [95], cast immobilization [96], and aging [97]. However, measures from muscle tissue homogenates cannot determine if the elevated purines arose from increased nucleotide degradation within the muscle fibers, or as a consequence of increased uptake of purines from the circulation, where uric acid increases are common during these, and many other, atrophy conditions [38].

Skeletal muscle is a heterogenous tissue containing many different cell types in addition to multinucleated myofibers, such as myogenic stem cells, mesenchymal progenitor cells, fibroblasts, adipocytes, immune cells, and endothelial cells [93]. Therefore, our ex vivo whole muscle experiments could not discern the cell type(s) in which purine nucleotide degradation was occurring. However, immunohistochemical staining of human and rodent skeletal muscle cross-sections show XOR expression is exclusive to non-muscle cell types such as vascular endothelial, smooth muscle, and

immune cells [43, 75]. These findings indicate that if purine nucleotide degradation was increased in the myofibers, synthesis of uric acid from myofiber purines would require their exchange with an adjacent XOR-expressing cell type. Our series of subsequent in vitro experiments demonstrated the feasibility of this scenario. First, we found that atrophy of multinucleated muscle cells (C2C12 myotubes) increased purine nucleotide degradation, which culminated predominantly in the release of hypoxanthine and xanthine, not uric acid. We then demonstrated that XOR-expressing cells readily convert exogenous hypoxanthine and xanthine to uric acid, which is prevented by the XOR inhibitor, allopurinol. Lastly, co-culturing myotubes with BAOEC (which express XOR), enabled the oxidation of myotube derived purines to uric acid, which was enhanced when the myotubes were undergoing atrophy.

Interestingly, our data suggests that the rapid oxidation of hypoxanthine and xanthine does not require uptake of these molecules into XOR expressing cells. The increased uric acid measured in the DEX treated C2C12+BAOEC co-cultures contained the same proportion of heavy-labeled uric acid as compared to the C2C12 only cultures. If the heavy labeled xanthine and/or hypoxanthine had been taken into the BAOEC cells, those molecules would have mixed with the unlabeled purine pool of the BAOEC, and any resulting uric acid would have a lower proportion of the label. The likelihood that myotube purines are oxidized extracellularly is further supported by the observation that XOR resides on the extracellular surface of BAOEC plasma membranes [98].

It is interesting that the atrophying EDLs and myotubes had increased purine nucleotide degradation despite ample access to exogenous nutrients and oxygen, and without any contractile demand. Increased skeletal muscle purine nucleotide degradation

and purine efflux are known to occur during conditions such as hypoxia and intense muscle contractions [35, 99], in which bioenergetic metabolism is unable to match rates of ATP synthesis with ATP hydrolysis. This leads to increased production of AMP and activation of AMPD in order to maintain the cellular energy state [36]. However, a downstream consequence of increased AMPD activity is increased purine nucleotide degradation and XOR activation in XOR-expressing cell types [37, 75, 100]. Therefore, our findings may reflect an ability of fasting, glucocorticoids, and FoxO to impair muscle bioenergetic function to an extent that resting ATP/ADP could not be maintained. This possibility is supported by NMR measurements of increased resting ADP concentrations, and decreased phosphocreatine and free energy of ATP hydrolysis (ΔGATP) in rat gastrocnemius muscle after dexamethasone treatment [101]. This would also explain why the EDLs had increased uric acid release without changes in AMPD 1/3, 5'NTC1a, and XOR expression.

On the other hand, FoxO mediated transcriptional upregulation of purine nucleotide degrading enzymes could have increased purine nucleotide degradation without increases in AMP/GMP/IMP levels. This possibility is supported by our findings of increased AMPD3 protein expression in TA muscles after fasting and DEX treatment, myotubes after DEX treatment and caFoxO3 expression, and our previous reports showing AMPD3 overexpression is sufficient to increase adenine nucleotide degradation in TA muscles and myotubes [81, 82].

The ability of DEX and caFoxO3 to increase AMPD3 protein expression likely stems from their activation of its promotor region activity and gene transcription, which we demonstrated to be dependent on the presence of FoxO binding sites. Previous

studies have also indicated the glucocorticoid receptor and FoxO transcription factors as regulators of AMPD3 gene expression [24, 102-104]. In C2C12 myotubes, Kuo et al. identified AMPD3 as one of 147 genes containing glucocorticoid binding regions in close proximity to their genomic sequence that was also upregulated by DEX treatment [102]. In human skeletal muscle, AMPD3 mRNA was upregulated by 4 days of oral DEX consumption [103]. Transgenic mice with a muscle specific knockout of all FoxO isoforms have attenuated AMPD3 mRNA upregulation in response to fasting and denervation induced atrophy [24], while overexpressing a dominant negative FoxO isoform attenuates AMPD3 mRNA upregulation in muscles during C26 carcinoma induced atrophy [104]. Our results in the present study build upon the numerous studies showing AMPD3 upregulation in atrophying muscle, by providing metabolic consequences (e.g. increased purine nucleotide degradation) to its upregulation. Moreover, given AMPD3 expression is controlled by glucocorticoids and FoxO, which are required for muscle atrophy in response to diverse set of upstream etiologies [18, 24, 28, 33, 105], our findings suggest that AMPD3-mediated increases in muscle purine nucleotide degradation is a common feature of muscle atrophy.

The results from this study may lend insight into targeting XOR as a therapy for many diseases and disorders. Treatment with XOR inhibitors such as allopurinol and febuxostat has been shown to have numerous therapeutic effects in humans and mice, such as improved endothelial function and reduced cardiovascular disease related incidents [40, 53, 59, 106], reduced adipose inflammation [61], hepatic steatosis and insulin resistance [56, 63], chronic kidney disease progression [55], cancer cachexia and mortality [54, 107], and disuse mediated muscle atrophy [67, 68]. Mechanistically, these

effects often are attributed to preventing oxidative stress caused by XOR produced superoxide anion, or adverse events related to high uric acid levels [63, 108-110] Our results suggest that muscle purine nucleotide degradation could be an upstream event leading to substrate driven increased XOR activity and various tissue pathologies. This may explain why the extent of muscle atrophy is a prognostic factor in many diseases [11, 111, 112]. Future studies examining the contribution of increased skeletal muscle purine nucleotide degradation to systemic XOR and peripheral tissue dysfunctions may lead to developing novel therapeutic strategies.

In conclusion, skeletal muscle purine nucleotide degradation and purine release are increased during atrophy and contribute to increases in serum UA. Mechanistically, glucocorticoids and FoxO3 increase muscle purine nucleotide degradation likely by upregulating AMPD3 expression. Muscle purine release is sufficient to drive increases in XOR activity and uric acid production by XOR-expressing cells. As such, preventing muscle purine nucleotide degradation could be a novel strategy for treating various pathologies associated with increased XOR activity and hyperuricemia.

TABLES AND FIGURES

	Low Performers (n=20)	Average Performers (n=20)	P value
Age (y)	51.1 ± 5.5	51.1 ± 5.9	>0.999
Height (cm)	162.6 ± 5.5	163.7 ± 5.9	0.528
Weight (kg)	75.1 ± 13.2	68.7 ± 9.5	0.086
BMI (kg/m^2)	28.4 ± 4.9	25.7 ± 4.0	0.664
App mass/height^2 (kg/m^2)	6.73 ± 0.91	6.87 ± 1.13	0.661
Grip Strength (kg)	17.0 ± 4.0	25.3 ± 2.6	**<0.0001**
Time to complete 5 sit-to-stands (s)	12.2 ± 1.7	9.0 ± 1.5	**<0.0001**
Number of sit-to-stand in 30 s	11.8 ± 1.5	15.7 ± 2.1	**<0.0001**
6 min Walk Distance (m)	490.4 ± 68.4	531.9 ± 65.1	0.060
Serum Creatine Kinase (IU/ml)	39.1 ± 16.8	40.7 ± 14.3	0.751
Serum Creatinine (mg/dl)	0.84 ± 0.15	0.83 ± 0.15	0.800

Table 2.1. Subject characteristics and performance measures. App mass = Appendicular Lean Mass. Mean ± SD. Statistical differences were determined by unpaired t-test.

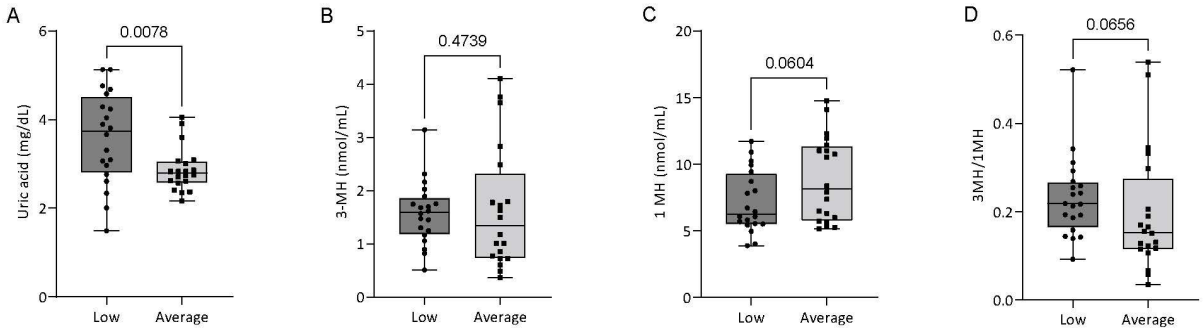

Figure 2.1. Serum uric acid is greater in individuals with below average physical fitness performance.

Serum was collected from adult women with either low or average physical performance. (A) Serum uric acid levels. (B) Serum 3-methylhistidine. (C) Serum 1-methylhistidine. (D) Ratio of serum 3-methylhistidine to 1-methylhistidine. n=20/group, unpaired t-test.

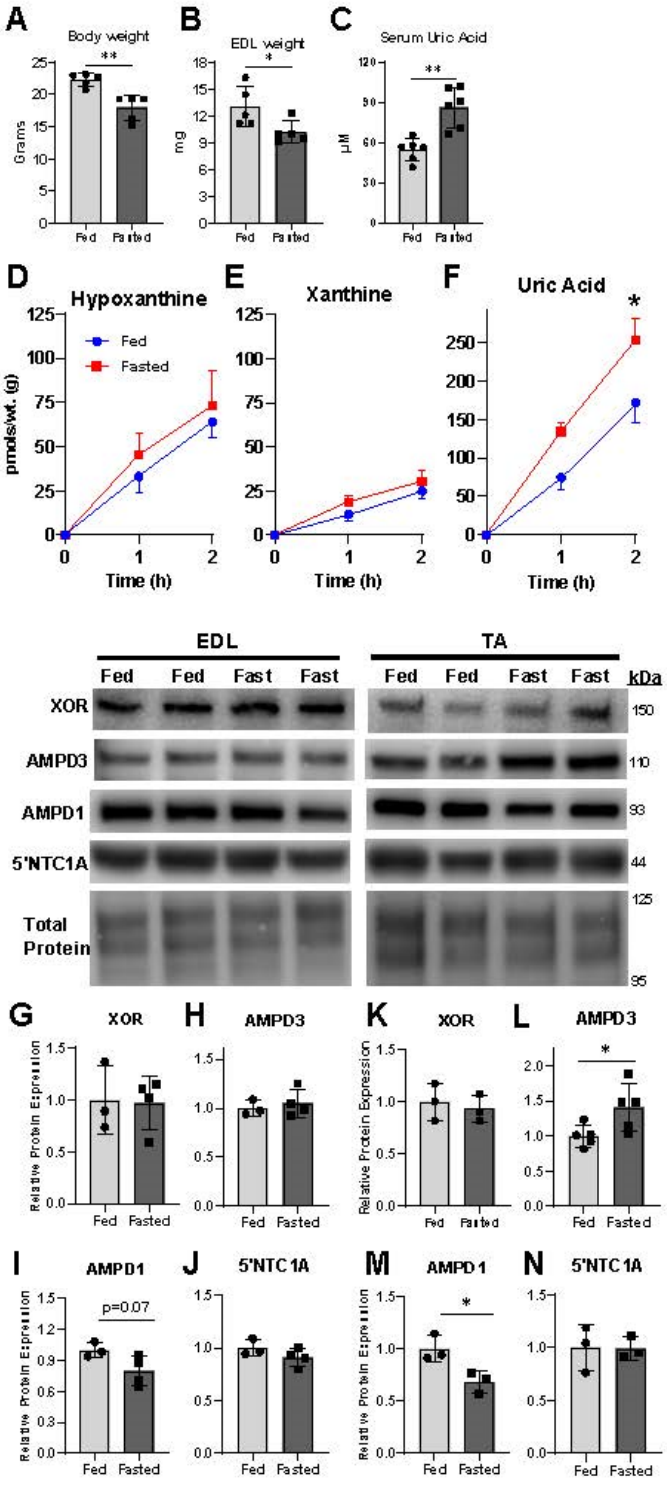

Figure 2.2. Fasting causes increased uric acid release from skeletal muscle.

Female C57BL/6J mice had food removed for 48 h. (A) Body weight of fed or fasted groups. (B) EDL muscle wet weights. (C) Uric acid concentration in serum collected at sacrifice. (D-F) Concentrations of the purine nucleotide breakdown products hypoxanthine, xanthine, and uric acid released from EDL muscles during ex vivo incubation. n=4-5/group, 2-way ANOVA Sidak's multiple comparisons test. *=p<0.001. (G-N) Protein expression levels of the purine nucleotide degrading enzymes xanthine oxidoreductase (XOR), AMP deaminases 1&3 (AMPD1/3), and cytosolic 5'nucleotidase 1 (5'NTC1A), from EDL (G-J) or tibialis anterior (TA) muscle (K-N). Panels A-C and G-N: two-tailed unpaired t-test, *=p<0.05, **=p<0.01.

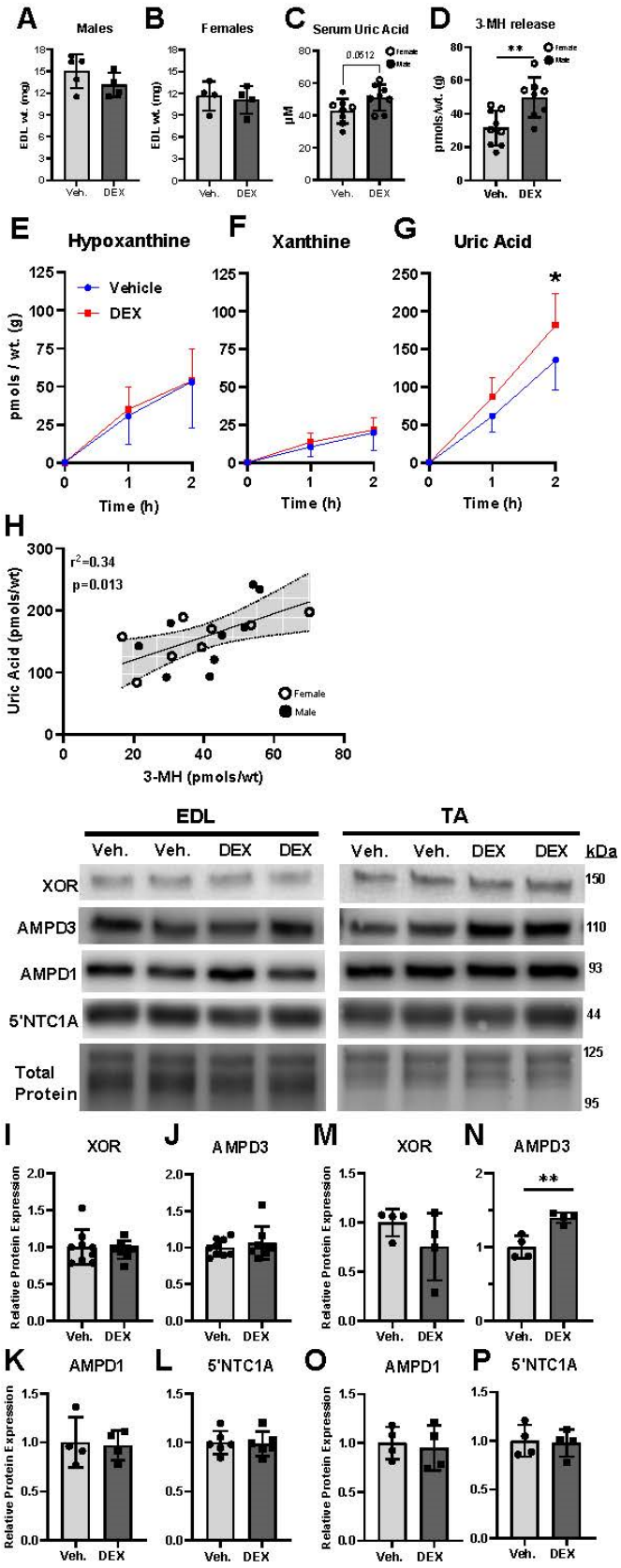

Figure 2.3. Glucocorticoid treatment is sufficient to increase uric acid release from skeletal muscle.
Male and female C57BL/6J mice were treated with subcutaneous injection of dexamethasone (DEX; 5mg/kg) or vehicle (Veh.) for 5 days. (A-B) Male or female EDL muscle wet weights after treatment period. (C) Uric acid concentration in serum collected at sacrifice. (D) Concentration of 3-methylhistidine (3-MH) measured in EDL incubation buffer after 2h. (E-G) Concentrations of the purine nucleotide breakdown products hypoxanthine, xanthine, and uric acid released from EDL muscles during ex vivo incubation. n=8/9 group combination of male & female, 2-way ANOVA Sidak's multiple comparisons. *=p<0.005. (H) Correlation between uric acid and 3-MH release from EDL muscles after 2h incubation period. (I-P) Protein expression levels of xanthine oxidoreductase (XOR), AMP deaminases 1&3 (AMPD1/3), and cytosolic 5'nucleotidase 1 (5'NTC1A), from EDL (G-J) or tibialis anterior (TA) muscle (K-N). Panels A-D and I-P: two-tailed unpaired t-test, **=p<0.01.

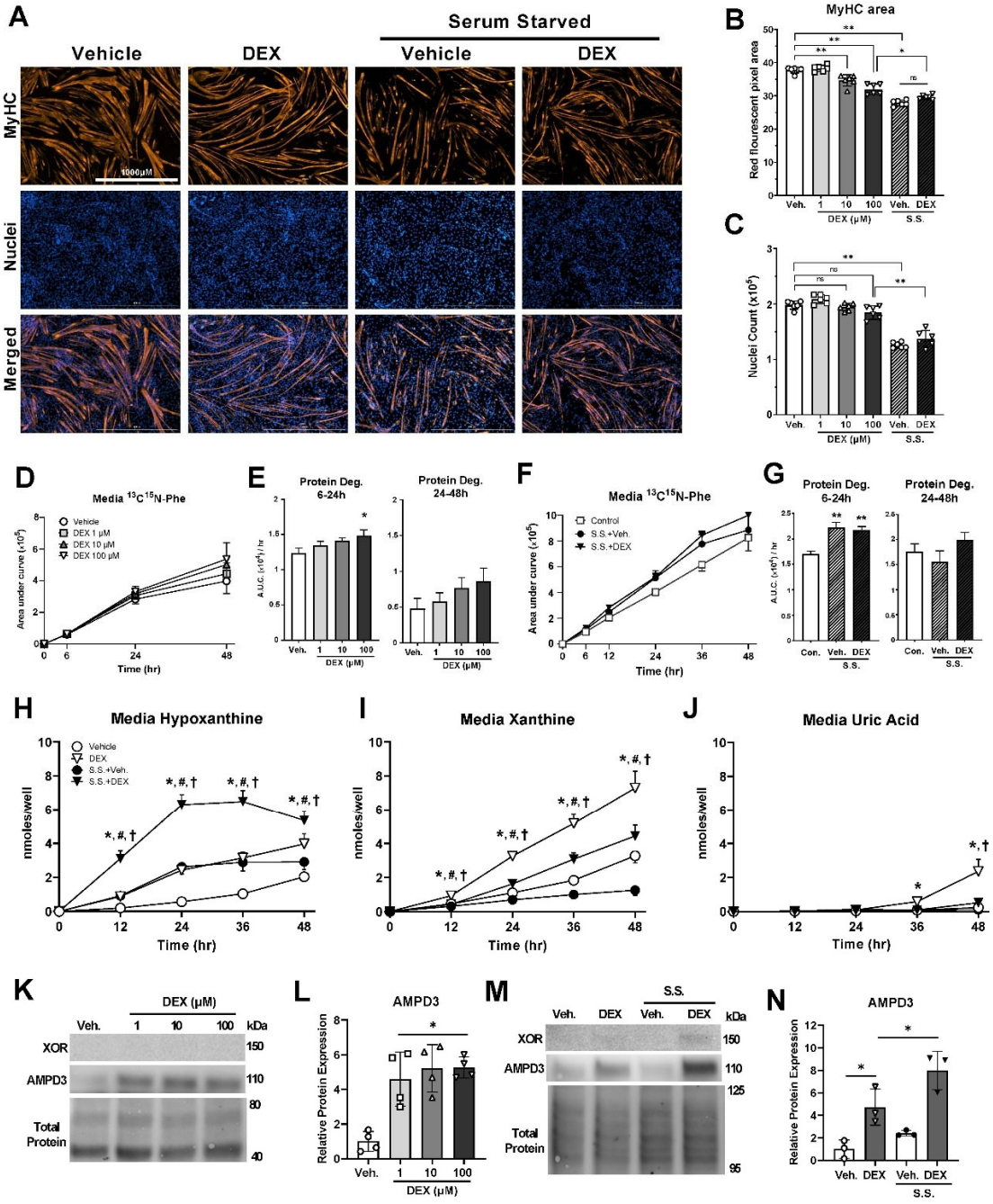

Figure 2.4. Purine nucleotide degradation is increased in atrophying myotubes but culminates in the release of hypoxanthine and xanthine due to their lack of XOR expression.

C2C12 myotubes were treated with dexamethasone (DEX) and/or serum starvation (S.S.) treatments for 48h. (A) Representative immunofluorescent images captured after staining for myosin heavy chain (MyHC) and nuclei (DAPI) in vehicle, 100μM DEX, S.S.+Veh., or S.S.+ 100μM DEX. (B-C) Quantifications of MyHC area and nuclei count per well. n=6 wells/condition and 100 images/well, *=p<0.05, **=p<0.01, 1-way ANOVA with Tukey's multiple comparisons. (D-G) Myotubes were differentiated in medium containing $^{13}C_9{}^{15}N$-phenylalanine to label cellular proteins, then washed with unlabeled media, and fresh unlabeled

media added for DEX treatment. (D) Media $^{13}C_9{}^{15}N$-phenylalanine release during DEX treatment. (E) Protein degradation rates determined by calculating the slopes between 6-24 and 24-48h media $^{13}C_9{}^{15}N$-phenylalanine. (F) Media $^{13}C_9{}^{15}N$-phenylalanine measured during S.S.+Veh., S.S.+ 100μM DEX, or untreated controls. (G) Protein degradation rates between 6-24 and 24-48h. Mean±SEM., n=6 wells/condition, *=p<0.05, **=p<0.001 vs veh/control, 1-way ANOVA with Dunnett's multiple comparisons. (H-J) Media concentrations of the purine nucleotide breakdown products hypoxanthine, xanthine, and uric acid during 100μM DEX and/or S.S. treatment. *=p<0.05 DEX vs Veh., # =p<0.05 S.S.+Veh. vs Veh., † =p<0.05 S.S.+Veh. vs S.S.+DEX 100μM. n=6 wells/condition, 2-way ANOVA with Tukey's multiple comparisons. (K-L) AMPD3 protein expression after 48h of DEX and/or S.S. treatments. *=p<0.05 vs. Veh. or indicated group.

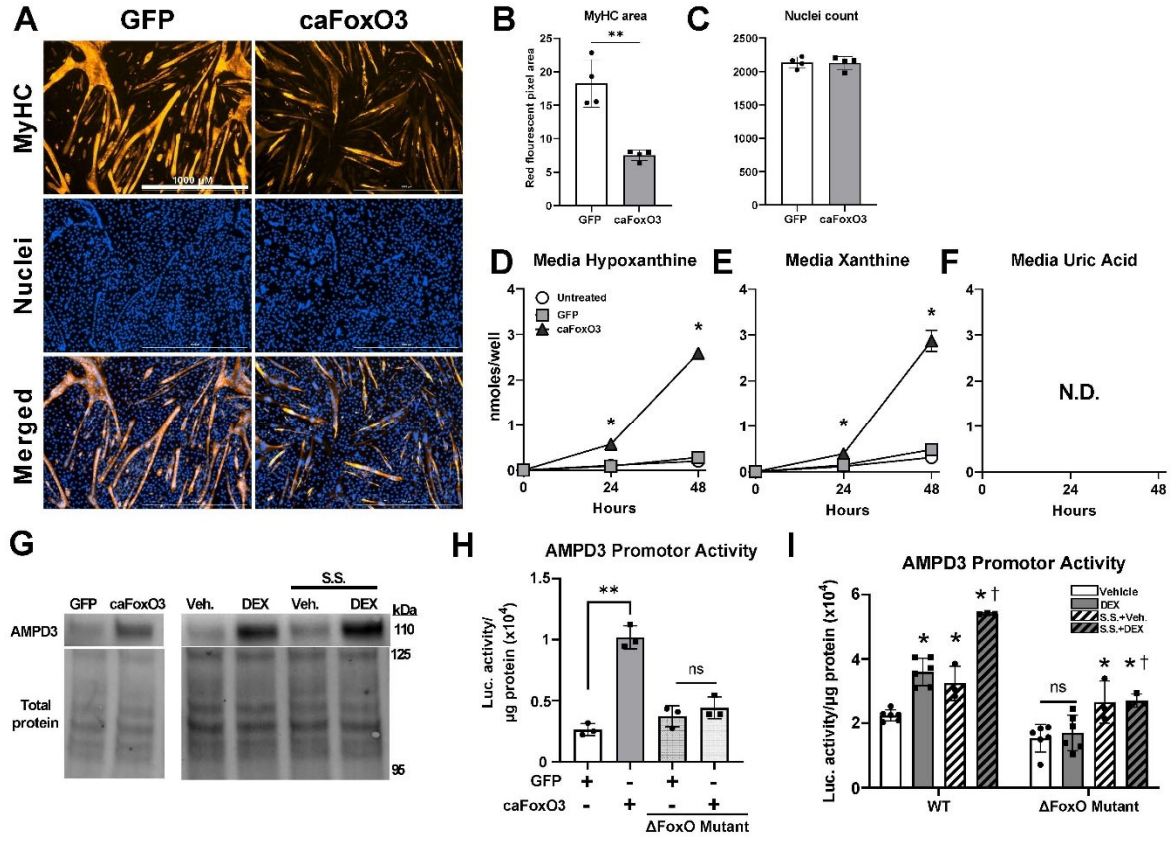

Figure 2.5. Increased FoxO3 activity is sufficient to induce myotube purine nucleotide degradation and is required for dexamethasone upregulation of AMPD3 promotor activity.

C2C12 myotubes were transduced with adenovirus encoding a constitutively active FoxO3 isoform (caFoxO3) or GFP for 48h. (A) Representative immunofluorescent images after staining for myosin heavy chain (MyHC) and nuclei (DAPI). (B-C) Quantification of MyHC area and nuclei count per well. n=4 wells/group and 6 random images/well. **=p<0.01. (D-F) Media concentrations of the purine nucleotide breakdown products hypoxanthine, xanthine, and uric acid. *=p<0.01 vs GFP. (G-H) Prior to differentiation, C2C12 myoblasts were transfected with luciferase reporter plasmids containing 1Kb of the AMPD3 proximal promotor region, with or without substitution mutations in the consensus FoxO binding site (ΔFoxO Mutant). (G) Western blots for AMPD3 after 24 h after GFP and caFoxO3 transduction or DEX and S.S. treatments. (H) AMPD3 promotor activity measured 24h after GFP or caFoxO3 transduction. 1-way ANOVA Tukey's multiple comparisons. **=p<0.0001. (I) AMPD3 promotor activity after 24h treatment with 100μM DEX and/or S.S.*=p<0.05 vs Veh, †=p<0.05 S.S.+DEX vs DEX. 2-way ANOVA Tukey's multiple comparisons.

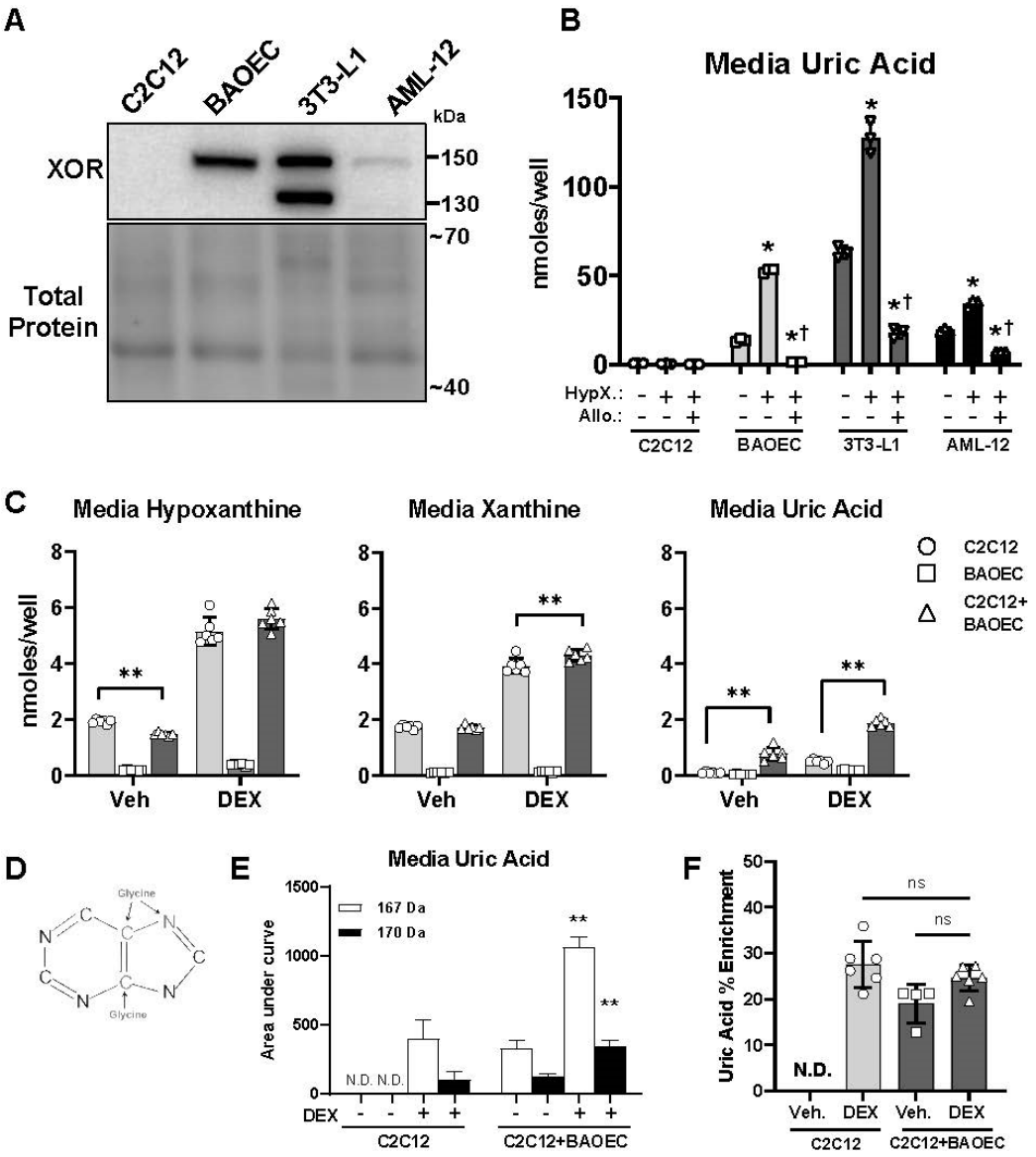

Figure 2.6. Xanthine oxidoreductase expressing cells oxidase exogenous purines released by muscle. (A-B) Myotubes (C2C12), aortic endothelial cells (BAOEC), adipocytes (3T3-L1), and hepatocytes (AML-12) were incubated with vehicle, 50μM hypoxanthine, or 50μM hypoxanthine + 100μM allopurinol (xanthine oxidoreductase inhibitor) for 48 h. Media samples were collected over time and purines were measured by UPLC. Cells were harvested for protein extraction and xanthine oxidoreductase (XOR) expression. (A) Western blots for XOR. (B) Media uric acid concentration after 48 h treatment. (C-F) C2C12 myotubes were grown in medium supplemented with $^{13}C^{15}N$-glycine to label purines. At day 5 differentiation, $^{13}C^{15}N$-glycine containing medium was replaced by normal medium containing vehicle or 100μM DEX, and given to wells with C2C12 myotubes only, BAOEC only, or C2C12+BAOEC co-cultures. (C) Media purine concentrations after 48 h. **=p<0.01, 2-way ANOVA Tukey's multiple comparisons test. (D) Uric acid illustration with atoms donated from glycine highlighted in red. (E) Media levels of normal (167 Da) vs. heavy-labeled (170 Da) uric acid from the same samples as C.**=p<0.01 vs C2C12 DEX. (F) Percentage of heavy-labeled uric acid per total uric acid measured. ns = not significant. N.D. = not detected. 1-way ANOVA Tukey's multiple comparisons.

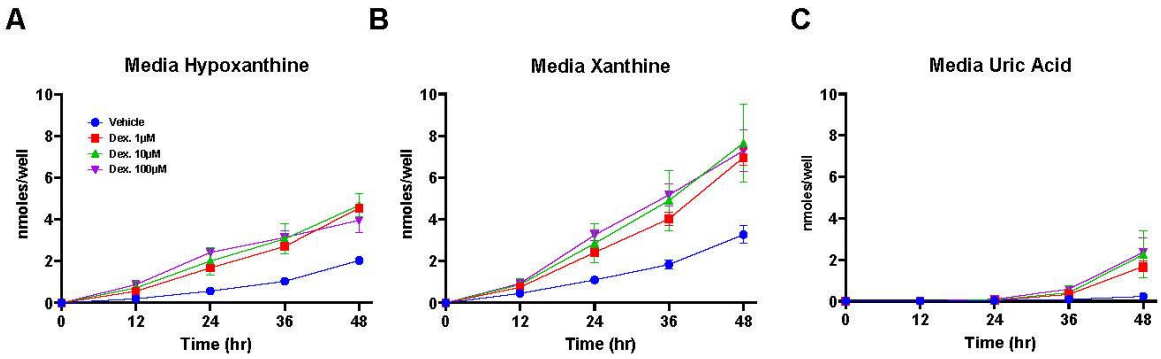

Supplemental Figure 2.1.
C2C12 myotube media concentrations of the purine nucleotide breakdown products hypoxanthine, xanthine, and uric acid during 48h treatment with vehicle, 1,10, 100μM DEX, and/or serum starvation (S.S.).

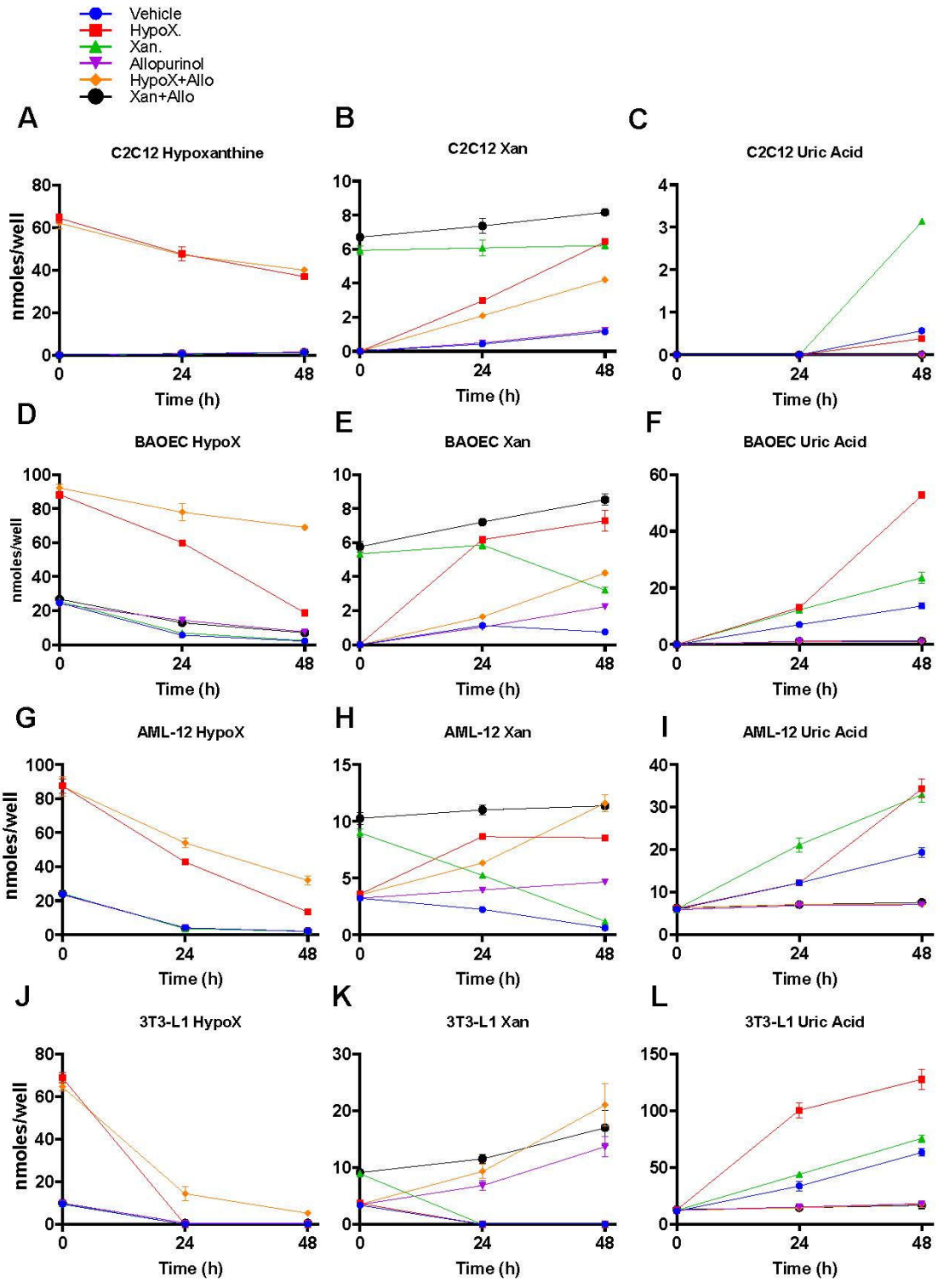

Supplemental Figure 2.2.
Media concentrations of hypoxanthine, xanthine, and uric acid in cultured myotubes (C2C12), aortic endothelial cells (BAOEC), adipocytes (3T3-L1), and hepatocytes (AML-12). Cells were treated for 48h with vehicle, 50μM hypoxanthine, 10μM xanthine, ± 100μM allopurinol, for 48 h.

CHAPTER 3

Uric acid exposure does not increase muscle protein degradation and atrophy of cultured skeletal muscle

ABSTRACT

Elevated serum uric acid is positively associated with sarcopenia and inhibition of xanthine oxidoreductase, the enzyme responsible for uric acid production, can partially attenuate muscle atrophy during various diseases and conditions. However, whether high levels of uric acid exposure are sufficient to induce muscle protein degradation and myotube atrophy are unknown. Here we utilized an in vitro model of multinucleated skeletal muscle cells, C2C12 myotubes, to address these unknowns. Exposing C2C12 myotubes to 175, 350, and 700 μM uric acid for 48 h did not affect myotube protein degradation rates or reduce total protein content. Additionally, combining 350μM uric acid with dexamethasone did not exacerbate increases in protein degradation or reductions in protein content. UPLC measures demonstrated myotubes were able to uptake uric acid, yet no differences in peroxiredoxin (PRX) dimerization were found, indicating it did not affect the cellular redox state. However, in keeping with its known antioxidant function, high levels of exogenous uric acid partially attenuated PRX2 hyperoxidation in response to exogenous H_2O_2 treatment. Collectively, these findings do not support a direct role for uric acid in the induction protein degradation and muscle atrophy.

INTRODUCTION

Skeletal muscle atrophy causes the loss of skeletal muscle mass and function that occurs during aging, disuse, diseases, and acute critical illness [1, 7, 113]. Given their importance for daily activity, respiration, and metabolic homeostasis, muscle atrophy has a number of negative consequences, such as reduced functional capacity and independence, metabolic disorders, psychological stress, and increased risk of mortality [3, 8, 9, 11, 13, 114]. Unfortunately, pharmacological therapies for preventing muscle atrophy are still unavailable, which highlights the importance of identifying novel mechanisms that contribute to muscle atrophy.

Elevated serum uric acid (UA) is a common feature of many diseases and conditions associated with skeletal muscle atrophy [38, 45, 48, 57]. Indeed, large scale population studies have found elevated serum uric acid to be positively correlated with sarcopenia [115, 116]. Uric acid is produced exclusively by the enzyme xanthine oxidoreductase (XOR), which catalyzes the oxidation of hypoxanthine and xanthine to UA, in the final step of purine nucleotide degradation in humans [38]. XOR inhibitors have been shown to significantly attenuate skeletal muscle atrophy in mice during disuse and cancer [54, 67-69], which has generally been attributed to the prevention of oxidative damage-induced protein degradation caused by XOR-generated superoxide anions. However, in muscle tissue, XOR is expression is found exclusively in the vascular endothelium, not skeletal muscle fibers [42, 43]. Interestingly, high UA alone has been reported to increase reactive oxygen species (ROS) and oxidative damage in various cell types [60, 61, 64], including C2C12 myotubes [70, 117]. Whether UA is sufficient to induce myotube protein degradation and atrophy remains unknown.

Therefore, the purpose of this study was to determine if UA is sufficient to increase muscle protein degradation and atrophy. To address this purpose, we exposed C2C12 myotubes to increasing levels of UA and measured the effect on protein degradation, oxidative stress markers, and total protein.

MATERIALS AND METHODS

Cell Culture

C2C12 mouse myoblasts (ATCC) were grown on gelatin-coated (Sigma G9391) 6-well plates in Dulbecco's modified Eagle's medium (DMEM) with 10% heat inactivated fetal bovine serum (Gibco 16140-071), and penicillin (100 IU/mL)/streptomycin (100 µg/mL). When myoblasts were 75-90% confluent, media was switched to differentiation media (DMEM with 2% horse serum (HS) and penicillin/streptomycin). Experiments were performed after 5 days of differentiation, with media refreshed every 48h and cells were maintained at 37°C and 5% CO_2. Uric acid (MP Biomedicals, 103215) was dissolved in fresh 1M NaOH to a stock concentration of 100mM after vigorous vortexing and warming to 37°C. Dexamethasone (MP Biomedicals, 190040) was dissolved in DMSO to a stock concentration of 100 mM. Volumes of 1M NaOH and DMSO equal to the highest experimental concentration given for vehicle control and preliminary experiments were conducted to confirm NaOH volumes were non-toxic. For H_2O_2 treatments, myotube media was replaced with serum free media containing indicated concentrations of H_2O_2 made by diluting 3% H_2O_2 stock (Sigma 88597) directly into warmed medium.

Media Purine and Amino Acid Quantification

Media samples were diluted 1:4 with cold (-20°C) 80% methanol, incubated at -20°C for 20 minutes, and then centrifuged for 10 min at 20,000xg and 4°C. An aliquot of supernatant was lyophilized using a Vacufuge plus (Cat 5305, Eppendorf) and resuspended in miliQ H_2O before analysis with Waters Acquity UPLC H-Class Bio system as done previously [118]. 3-methyl histidine levels were measured using derivatization of amine groups using the AccQ-Tag kit (SKU 186003836, Waters, Milford, MA, USA), according to manufacturer instructions, with 70 µL of borate buffer, 15 µL of sample, and 15 µL AccQ-Tag Ultra reagent. Separation was performed on Waters Acquity UPLC H-Class Bio system.

Degradation Rates of Long-Lived Proteins

C2C12 myoblasts differentiated in DMEM with 2% HS, 1% PenStrep, and $^{13}C_9{}^{15}N$-Phenylalanine (130 mg/L, Sigma #608017). Five days later, myotubes were washed twice with normal unlabeled DMEM, with additional washes repeated 1 and 2 h later to allow degradation of short-lived proteins. After the second chase period, treatments were initiated and media samples were collected over time for measurement of $^{13}C_9{}^{15}N$-Phenylalanine by UPLC-mass detection (Water Acquity QDa).

Peroxiredoxin Dimerization Analysis

Detection of peroxiredoxin dimers and monomers for estimating the cellular redox state was done according to established protocols [119]. After experimental treatments, myotubes were washed twice with ice cold Phosphate Buffered Saline (PBS) that was pre-incubated with 10ug/ml catalase (Sigma C1345) for 1h. Following washes, myotubes were incubated for 10 min. on ice with ice-cold 100mM N-Ethylmaleimide (NEM, Sigma

04259) dissolved in 1x PBS. Myotubes were then harvested in RIPA buffer (1xPBS, 1% NP-40, 0.5% sodium deoxycholate, 0.1% SDS, 100mM NEM, protease and phosphatase inhibitors (Roche)). Proteins (10μg) were separated by non-reducing SDS-PAGE.

Western Blot Protein Analysis

Myotubes were harvested in RIPA buffer (1xPBS, 1% NP-40, 0.5% sodium deoxycholate, 0.1% SDS, protease and phosphatase inhibitors (Roche)) and lysates were rotated end over end for 1h at 4°C. Lysates were centrifuged at 20,000xg for 10 min at 4°C, and supernatant fraction containing solubilized proteins was retained and protein concentration was determined by BCA Assay (Pierce). Proteins (10-15μg) were separated by SDS-PAGE (7.5-12% BioRad TGX stain-free gels) then transferred to polyvinylidene difluoride (PVDF) membranes. Equal loading and transfer of proteins was confirmed by capturing protein fluorescence after photoactivation of gels and membranes. Membranes were blocked for 1 h at room temperature using a 5% bovine serum albumin (BSA, Sigma A7906) dissolved in Tris buffered saline with 0.1% tween 20 (TBS-T) solution. Primary antibodies were diluted in TBS-T+2-5% BSA and incubated with membranes overnight at 4°C with rocking. Secondary antibodies conjugated to horseradish peroxidase (Cell Signaling #7074, ThermoFisher #31444) were diluted 1:5000 in TBS-T+2%BSA and incubated with membranes at room temperature for 1 h. Proteins were detected using Western Chemiluminescence HRP Substrate (EMD Millipore). Band intensities were captured using a Bio-Rad Chemi Doc XRS imager and analyzed using Image Lab Software 6.1 (Bio-Rad). Approximate molecular weights of protein were calculated relative to PageRuler Plus protein ladder (ThermoFisher). Primary antibodies used were PRX2 (Abcam ab109367), PRX3 (Abcam

ab73349), phospho-p38 MAPK (Thr 180/Try182) (Cell Sig. #4511), p38 MAPK (Cell Sig. #9212).

Statistics

All data are presented as mean ± standard deviation. Statistical significance was determined by one-way ANOVA with Tukey's or Sidak's multiple comparisons. All data were tested for equal variance using Browns-Forsythe test and Gaussian distribution using Anderson-Darling test. If data were normally distributed, values were log transformed and reanalyzed. Statistical analyses were conducted using GraphPad Prism Software (9.3) and p-values less than 0.05 were considered significant. All experiments were repeated at least twice to confirm reproducibility.

RESULTS

Exogenous uric acid exposure does not increase myotube protein degradation or cause atrophy

To determine if increased UA exposure increases muscle protein degradation, we measured protein degradation rates in C2C12 myotubes exposed to 175, 350, or 700μM UA (amounts corresponding to normal, high, and hyperuricemic values in human serum), for 48 hours. As a positive control, we included treatment with the synthetic glucocorticoid dexamethasone (DEX) [120], and, to elucidate if UA could exacerbate DEX mediated protein degradation, a DEX + 350 μM UA treated group. As expected, overall protein degradation rates were increased by DEX during the first 24 h of treatment (Fig. 3.1A-C). However, no differences in 0-24 or 24-48 h protein degradation rates were observed between vehicle or UA treated groups (Fig. 3.1A-C). Moreover, DEX+350 μM UA did not

exacerbate the increase in protein degradation caused by DEX (Fig. 3.1A-C). Further, UA did not increase release of 3-methylhistidine, which is also an indicator of myofibrillar protein degradation [121] (Fig. 3.1D). In agreement with these measures, total protein content was similar between vehicle and UA treated, and decreased similarly in DEX and DEX+350 μM UA groups (Fig. 3.1E).

Exogenous uric acid does not increase oxidative stress in myotubes

To determine if exogenous UA causes oxidative stress in muscle cells, we measured the dimerization status of peroxiredoxin isoforms 2 and 3 (PRX 2/3) after 48h UA exposure. Peroxiredoxins are a family of ubiquitously expressed peroxidases, which contain a conserved cysteine residue capable of reducing H_2O_2. In the reaction, a PRX cysteine is oxidized to sulfenic acid which can then forms a disulfide bond with a non-oxidized cysteine residue on another PRX monomer, yielding temporarily stabilized PRX dimers. Thus, the cellular redox state can be determined by quantifying the ratio of PRX dimers to the sum of PRX dimers and monomers using immunoblot analysis [119]. No differences were detected in PRX2 (cytosolic) (Fig 3.2A-B) or PRX3 (mitochondrial) (Fig 3.2C-D) dimerization between vehicle and UA treated groups. In agreement with these findings, no differences were detected in the phosphorylation of p38 MAPK, which is an oxidative stress sensing kinase [122].

Uric acid is not degraded and moderately taken up by myotubes

A possible explanation for the lack of UA effects on myotube protein degradation and redox state is that it is degraded or unable to be consumed by the myotubes. Therefore, media UA was measured at the start of treatments and after 48 h. Media UA

concentrations at time 0 matched the calculated doses given, and remained stable throughout the 48 h period (Fig. 3.3A), suggesting that UA was not consumed over time. However, cellular UA increased significantly after 48h exposure to 350 μM UA (Fig. 3.3B), suggesting that some UA is taken up by the myotubes.

Exogenous uric acid partially attenuates H_2O_2 oxidative stress

Given that media UA remained elevated throughout the 48h treatment period, and UA is a major circulating antioxidant due to its ability to react with numerous reactive oxygen species [123], we next tested whether extracellular UA could attenuate exogenous H_2O_2 mediated oxidative stress. Under conditions of high H_2O_2 concentrations, the PRX active site cysteine will undergo hyperoxidation to sulfinic or sulfonic acid [124]. These hyperoxidized PRX monomers are unable to form disulfide bonds, resulting in an accumulation of PRX monomers when cells are exposed to high levels of H_2O_2 [125]. In preliminary experiments, we found exposing C2C12 myotubes to 50 or 150 μM H_2O_2 for 10 minutes, had no effect on PRX2 dimer abundance (Fig. 3.4A). On the other hand, 500 μM H_2O_2 was sufficient to deplete PRX2 dimers and increase PRX2 monomers, indicating PRX2 hyperoxidation (Fig. 3.4A). We then tested whether UA could attenuate this effect by co-incubating the myotubes with 500 μM H_2O_2 and 700 μM UA. While the addition of UA did not attenuate H_2O_2 mediated increases in PRX2 monomers (Fig. 3.4C), it did partially preserve levels of PRX2 dimers (Fig. 3.4D), and the ratio of PRX2 dimers to total PRX2 (Fig. 3.4E). This effect was specific for cytosolic PRX2, as no differences in monomer, dimer, or dimer/total intensities were observed for the mitochondria localized PRX3 isoform (Fig. 3.4F-I).

DISCUSSION

Elevated serum UA is common in muscle atrophy associated conditions and independently associated with sarcopenia in humans [38, 115]. In this study we tested whether exogenous UA could directly increase skeletal muscle protein degradation and atrophy. We found no differences in C2C12 myotube protein degradation rates, 3-methylhistidine release, or total protein content, after 48h treatment with 175, 350, and 700μM UA. Moreover, despite confirming that the myotubes were able to uptake UA, we did not find increased levels of cytosolic and mitochondrial PRX dimerization, which is a sensitive marker for increased H_2O_2 concentrations. In contrast, high levels of UA lessened PRX hyperoxidation in response to H_2O_2 administration, which supports UA's known role as an antioxidant.

Despite high serum UA being an independent predictor of sarcopenia [115], and the ability of XOR inhibitors to preserve muscle mass during disuse and cancer-induced muscle atrophy [54, 67-69], few studies have examined the direct effects of UA on skeletal muscle cells. Yuan et al. found increased ROS and reduced insulin stimulated AKT phosphorylation in C2C12 myotubes treated with 15 mg/dL (892 μM) UA for 24 h [117]. Maarman et al. found that C2C12 myotubes exposed to 750 μM UA for 72h had increased markers of lipid peroxidation and impaired electron transport chain complex II activity [70]. Oxidative damage, impaired insulin signaling, and mitochondrial dysfunction are all implicated as playing causative roles in the induction of muscle protein degradation and atrophy [71]. Nevertheless, this study clearly demonstrates that protein degradation is not increased in skeletal muscle cells when exposed to high UA levels in vitro. Therefore, the findings that XOR inhibitors can protect against disuse and cancer induced muscle atrophy are not likely explained by direct effects of UA on skeletal muscle fibers.

However, in an in vivo setting, high levels of UA may be sufficient to increase muscle protein degradation via several indirect mechanisms. For example, monosodium urate crystals, which can form when serum UA levels near/exceed its solubility limit of 405 μmol/L (6.8 mg/dL)[126], are known to directly activate the NLRP3 inflammasome in immune cells [127]. This increases production of IL-1β, a proinflammatory cytokine shown to increase muscle protein degradation and atrophy [128]. Further, high UA may directly cause of vascular endothelial dysfunction and reduced nitric oxide bioavailability [108, 129], which are implicated to promote muscle atrophy during periods of disuse and aging [130, 131]. UA has been shown to stimulate monocyte chemoattractant protein 1 (MCP-1; also known as CCL2) expression and/or excretion from rat vascular smooth muscle cells [132], and 3T3-L1 adipocytes [61]. This chemokine promotes macrophage infiltration into tissues and is a biomarker for cachexia in pancreatic cancer patients [133]. Thus, future studies to test whether UA can indirectly stimulate muscle atrophy in vivo are warranted. It should be noted, however, that increasing UA levels in rodents through knockdown or inhibition of urate oxidase causes time-dependent renal dysfunction, systemic inflammation, and β-cell death [134, 135]. Therefore, in vivo studies using rodents would need to control for confounding variables in order to determine the specific effects of increased serum UA on muscle mass.

In apparent contrast to our findings that UA did not increase PRX 2/3 oxidation, previous studies have reported high UA exposure (concentrations ranging 500-892 μM) causes increased in ROS and/or oxidative damage in HUVEC endothelial cells [64], HepG2 hepatocytes [60], 3T3-L1 adipocytes [62], and C2C12 myotubes [70, 117]. In general, these effects were attributed to elevated mitochondrial superoxide anion

production. In all cell types, superoxide dismutase rapidly converts superoxide to H_2O_2, which, in turn, is predominantly degraded by PRX oxidation [136]. In the majority of the previous studies, ROS levels were detected using fluorescent probes such as DCFH and MitoSOX, which detect many different types of ROS, but not H_2O_2 [137]. Therefore, because H_2O_2 is the primary ROS detected by PRXs, the differences in our results may be related to the ability of UA to increase ROS other than H_2O_2.

Additionally, the sensitivity of different cell types to any effects of exogenous UA is likely dependent on their capacity for its uptake. Virtually all of the previous studies that have examined the effects of high UA exposure have used cell types that have abundant XOR expression [41] and, thus, would be expected to express primary UA transporters, URAT1 (SLC22A12) and GLUT9 (SLC2A9) [138] at greater levels than skeletal muscle cells, which do not express XOR [43]. Indeed, URAT1 and GLUT9 mRNA and/or protein expression have been detected in 3T3-L1 and mouse adipocytes [62, 139], and HUVEC endothelial cells [140], and HepG2 hepatocytes [141] but have not been reported in skeletal muscle or C2C12 myotubes. Therefore, differences in the capacity for UA uptake may be an underlying factor between differences in sensitivity to high UA between cell types.

In conclusion, UA exposure does not influence protein degradation or cause muscle atrophy in C2C12 myotubes. Although previous reports show high exogenous UA to increase superoxide production and ROS levels in various cell types, we found that it does not increase H_2O_2 sensitive redox markers in C2C12 myotubes. In contrast, it partially protected against H_2O_2-mediated oxidative stress. Therefore, the independent association between high serum UA and sarcopenia, and the ability for XOR inhibitors to

protect against muscle atrophy, are unlikely due to direct effects of UA on skeletal muscle fibers.

TABLES AND FIGURES

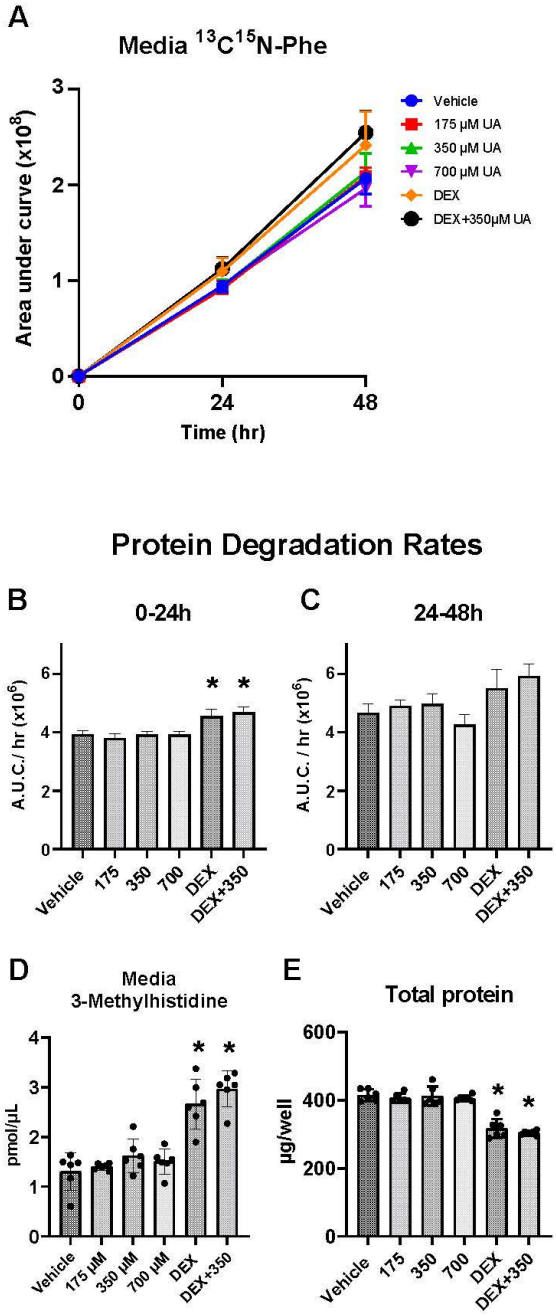

Figure 3.1. Exogenous uric acid exposure does not increase myotube protein degradation or cause atrophy. C2C12 myotubes were allowed to differentiate for 5 days in media supplemented with $^{13}C_9{}^{15}N$-phenylalanine to label cellular proteins. At day 5, myotubes were given normal media containing the indicated doses of uric acid (U.A.) and/or dexamethasone (DEX) for 48 h. (A) Media levels of $^{13}C_9{}^{15}N$-phenylalanine measured in media collected at 0, 24, and 48 h post U.A. and/or DEX treatment. (B) Protein degradation rates calculated from slope changes in media $^{13}C_9{}^{15}N$-phenylalanine. C) Media concentrations of 3-methylhistidine (3-MH). (D) Total protein per well after 48 h. n=6wells/condition, Mean±S.D., * = $p<0.05$ vs. vehicle, one-way ANOVA Sidak's multiple comparisons.

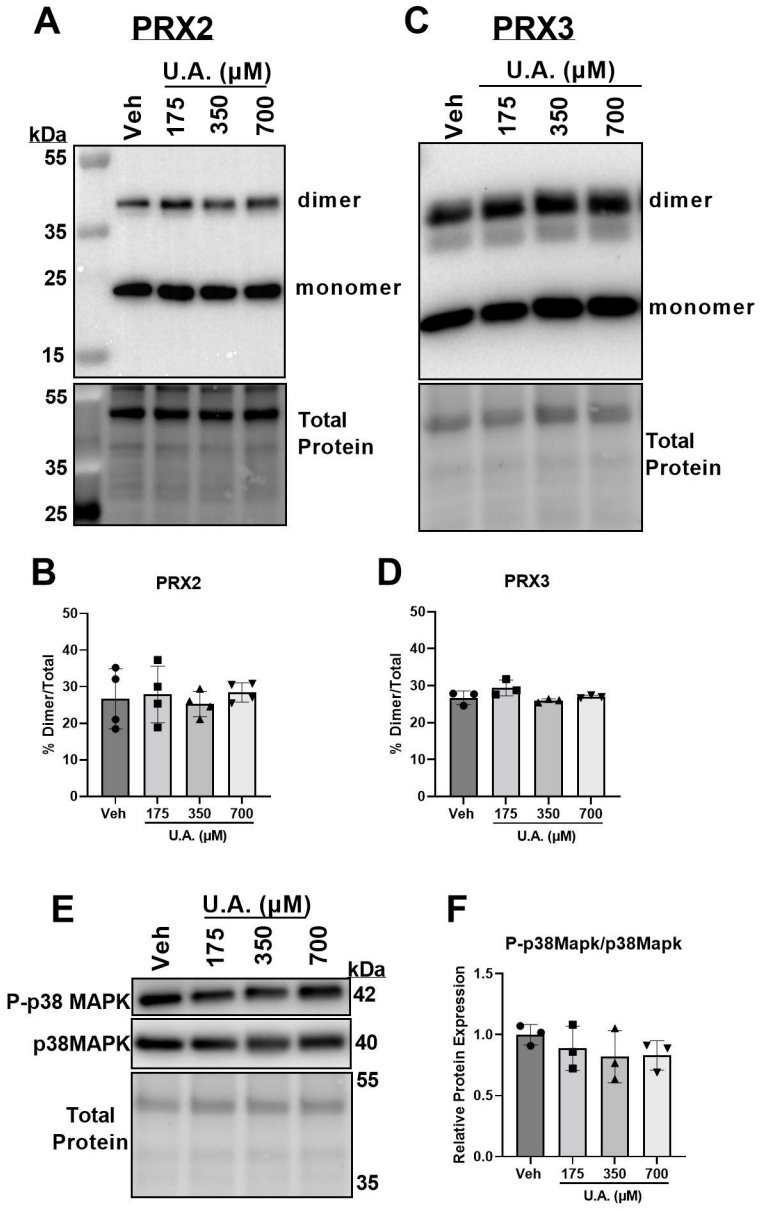

Figure 3.2. Exogenous uric acid exposure does not increase oxidative stress in myotubes. Myotubes were treated exactly as in indicated Fig.1. After the 48 h treatment period, myotubes were harvested for immunoblot analysis of PRX2 (cytosolic) and PRX3 (mitochondrial) dimerization. (A) Immunoblot images for PRX2 dimers and monomers. (B) Percentage of PRX2 dimers per total PRX2 (dimers+monomers). (C) Immunoblot images for PRX3 (mitochondrial) dimers and monomers. (D) Percentage of PRX3 dimers per total PRX3. (E) Immunoblot images for phosphorylated p38 MAPK (Thr180/Tyr182) and total p38 MAPK. (F) Quantification of P-p38MAPK/p38MAPK. n=3-4 wells/condition, Mean±S.D., one-way ANOVA Sidak's multiple comparisons.

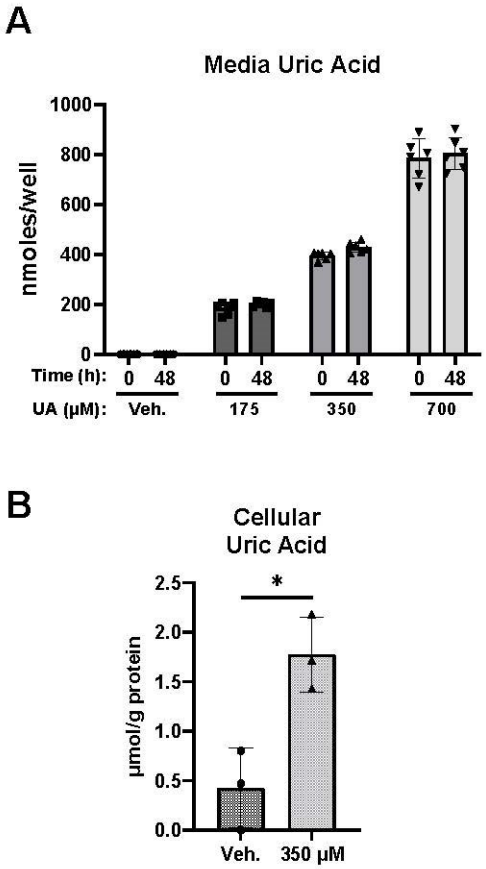

Figure 3.3. Exogenous uric acid does increase myotube intracellular uric acid. C2C12 myotubes were allowed to differentiate for 5 days and then treated with U.A. (A) Media U.A. concentrations measured immediately after treatment start and 48 h later. (B) Intracellular U.A. concentrations measured after the 48 h treatment period. n=3-6 wells/condition, Mean±S.D.

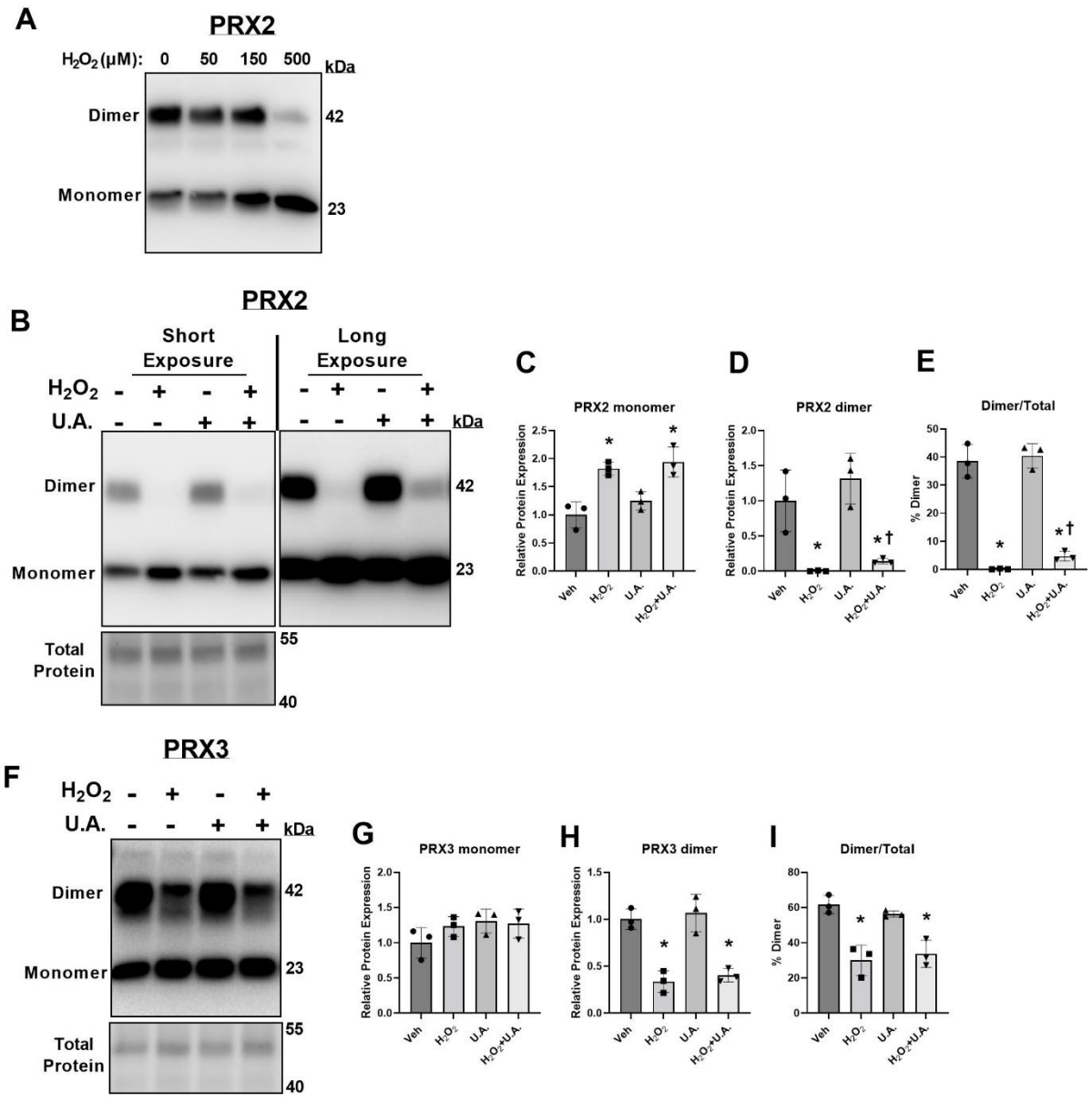

Figure 3.4. Exogenous uric acid partially attenuates H_2O_2 mediated oxidative stress. C2C12 myotubes were allowed to differentiate for 5 days. (A) Immunoblot images for PRX2 monomers and dimers after 10 min. treatment with 0, 50, 150, or 500 μM H_2O_2. (B) Immunoblot images and densitometry analysis (C&D) of PRX2 monomers and dimers after 10 min. treatment with or without 500μM H_2O_2 ± 700μM U.A. Densitometry analysis was conducted on low exposure images. (E) Percentage of PRX2 dimers per total PRX2. (F) Immunoblot images and densitometry analysis (G&H) of PRX3 monomers and dimers. (I) Percentage of PRX3 dimers per total PRX3. n=3 wells/condition, Mean±S.D., *=p<0.05 vs. vehicle, †=p<0.05 vs. H_2O_2, one-way ANOVA Sidak's multiple comparisons.

CHAPTER 4

Discussion

Summary of Major Findings

Increases in UA production and serum UA are both implicated to promote the development and progression of various disorders and chronic diseases [40, 59-61, 74]. Atrophy of skeletal muscles is highly prevalent in conditions of elevated XOR activity and serum UA, and widely reported to involve a reduction in muscle adenine nucleotide concentrations and increased expression of an adenine nucleotide degrading enzyme [38]. However, whether purine nucleotide degradation is increased in atrophying muscle and contributes to elevated UA production and serum UA are unknown. Moreover, although high serum UA is independently associated with sarcopenia [115], and XOR inhibitors can protect against muscle atrophy [54, 67-69], the ability for UA to directly cause muscle atrophy is unknown.

In Chapter 2 of this dissertation, we found fasting and treatment with the synthetic glucocorticoid dexamethasone (DEX) increased mouse serum UA levels and UA efflux from atrophying EDL muscles. In C2C12 myotubes, DEX and caFoxO3 caused increased AMPD3 protein expression and hypoxanthine and xanthine efflux. The DEX- and caFoxO3-mediated increases in AMPD3 expression coincided with their activation of its promotor region, which was dependent on FoxO binding. Increased purine nucleotide degradation in myotubes, however, produced little to no UA owing to their lack of XOR expression. When myotubes were co-cultured with endothelial cells, which express XOR, DEX treatment increased UA production solely from myotube released purines. These findings demonstrate that glucocorticoids increase purine nucleotide degradation in

skeletal muscles which contributes to increases in serum UA. Mechanistically, glucocorticoid-mediated skeletal muscle purine nucleotide degradation likely involves FoXO-dependent transcriptional upregulation of AMPD3 in skeletal muscle fibers. In turn, increased muscle fiber purine nucleotide degradation and purine release stimulate UA production by adjacent XOR-expressing cells.

In Chapter 3, we found that exposing C2C12 myotubes to UA does not increase protein degradation rates or cause loss of protein content. UPLC analysis confirmed that media UA levels were maintained at the calculated doses over the 48h treatment period, and resulted in a 3-fold increase in intracellular UA concentration. In agreement with its lack of effect on protein degradation, UA did not increase the dimerization of peroxiredoxins 2 & 3, or the levels of phosphorylated p38-MAPK, suggesting it did not affect the cellular redox state. In contrast, UA partially attenuated the hyperoxidation of PRX2 in response to excessive H_2O_2 levels, which agrees with the known role of UA as a major antioxidant. These findings indicate that high UA exposure does not directly increase skeletal muscle atrophy. Therefore, the association between high serum UA and sarcopenia, and the ability for XOR inhibitors to protect against muscle atrophy, are unlikely due to direct effects of UA on skeletal muscle fibers

Cellular mechanisms underlying increased muscle purine nucleotide degradation

Increased rates of adenine nucleotide degradation in skeletal muscle are best documented during intense muscle contractions and hypoxia, conditions in which ATP hydrolysis outpaces ATP synthesis [35, 100]. In such conditions, the combined reactions of adenylate kinase (ADP + ADP $\leftrightarrow$ ATP + AMP) and AMP deaminase (AMP $\rightarrow$ IMP + NH_3) help to preserve the free energy of ATP hydrolysis but lead to increased IMP

degradation and purine efflux. Increased activity of AMPD in these situations occurs rapidly and is driven by increases in AMPD substrate levels (e.g. AMP) and reduced allosteric inhibition [142]. When muscle contractions cease, IMP production also stops, and the adenine nucleotide pool (ATP + ADP + AMP) is replenished by its amination to AMP (IMP→ sAMP→ AMP) [143].

In Chapter 2, our findings of increased purine efflux from atrophying muscles and myotubes, despite ample oxygen and nutrients, may reflect an ability of fasting, glucocorticoids, and FoxO to increase energy demand or impair bioenergetic function to an extent that resting ATP/ADP could not be maintained. In vivo NMR measurements have shown increased resting ADP concentrations, decreased phosphocreatine concentration, and decreased calculated free energy of ATP hydrolysis (ΔG_{ATP}) in rat gastrocnemius muscle after dexamethasone treatment [101]. This would agree with the findings that uric acid efflux from atrophying EDL muscles was increased despite unchanged protein expression of AMPD 1/3, 5'NTC1a, and XOR.

On the other hand, increased AMPD3 protein expression by FoxO mediated upregulation of its gene could be the sole mechanism underlying increased purine nucleotide degradation, i.e. a mismatch in ATP supply/demand may not be required. We have previously found overexpression of this AMPD isoform in TA muscles and C2C12 myotubes to be sufficient to increase adenine nucleotide degradation and purine efflux [81, 82]. Given that it is upregulated in atrophying muscles during various diseases [30], disuse [31], and aging [32], it is likely that this was the mechanism underlying our observations.

Physiological roles for glucocorticoid control of muscle purine nucleotide degradation

The DEX-mediated increases in uric acid efflux from mouse EDL muscles and DEX induced increase in hypoxanthine and xanthine release from C2C12 myotubes demonstrate that glucocorticoids regulate skeletal muscle purine nucleotide degradation and purine release. Endogenous production of the glucocorticoid cortisol, corticosterone in rodents, is upregulated in response to a variety of physiological stress conditions in which exogenous nutrients are insufficient for systemic energy demands. This includes conditions such as starvation and malnutrition, chronic diseases, infections, or traumatic injuries [144]. Glucocorticoids, which are sufficient to induce muscle wasting [19], are able to maintain metabolic homeostasis by controlling metabolism and gene expression in key metabolic tissues such as the liver, adipose, and skeletal muscle. For example, they maintain blood glucose levels by stimulating hepatic gluconeogenesis and skeletal muscle de novo alanine synthesis and release to support hepatic gluconeogenesis [145]. Additionally, they upregulate skeletal muscle glutamine synthetase and de novo glutamine synthesis to support glutamine demand by immune or intestinal cells [146, 147].

Interestingly, while there are several examples for glucocorticoid control of glucose, amino acid, and lipid metabolism, their ability to regulate nucleotide metabolism is unknown. Skeletal muscles are not only the most abundant tissue by mass in the body but contain the highest concentrations of free purine nucleotides [76] and enzymatic capacity to synthesize purine nucleotides [77]. As such, our observations that glucocorticoids upregulate muscle purine nucleotide degradation and purine release may

be part of broader physiological mechanism by which systemic demand for purines is met during stress conditions. Furthermore, skeletal muscle fibers lack of XOR expression could be connected to its proposed role as an endogenous purine reservoir. XOR oxidation of hypoxanthine and xanthine is irreversible and decreases salvageable purines. The lack of XOR expression by muscles may function to ensure that it does not simultaneously generate and remove purines.

Alternatively, glucocorticoid-induced muscle purine nucleotide degradation may serve to maintain antioxidant levels. Uric acid is the major circulating antioxidant in humans [123, 148]. Since glucocorticoids are increased during many stress conditions that are coincident with muscle atrophy [149], the release of uric acid precursors from muscle may allow antioxidant capacity to other tissues.

Targeting muscle purine nucleotide degradation pathway for therapies

Skeletal muscle atrophy is highly prevalent in diseases and conditions in which elevated XOR and high UA are implicated in the development and poor prognosis. Treatment with inhibitors of XOR has been shown to have several positive outcomes such as improved endothelial function and blood flow, atherosclerosis, and other cardiovascular disorders [40, 53, 59, 106], reduced adipose tissue inflammation [61], hepatic steatosis and insulin resistance [56, 63], and gouty arthritis [126]. Mechanistically, the positive effects of XOR inhibitors are generally attributed to preventing oxidative stress caused by XOR produced superoxide anions or aberrations directly related to high uric acid levels [40, 63, 108-110]. However, XOR inhibitors have some major side effects that make more targeted approaches attractive [57, 58]. This dissertation suggests two possible approaches to improve specificity. First, since muscle atrophy is common in

many of these diseases, targeting XOR inhibitors to muscle tissue (e.g. vascular cells in muscle) may limit side effects that occur in other tissues. Second, a seemingly unappreciated consequence of accelerated nucleotide degradation is the decrease in ATP content [81, 82]. Given the importance of ATP content for many cellular functions [38, 150], we propose that the positive effects of XOR inhibition may be in the slowing of ATP depletion of muscle. Therefore, targeting therapies to directly protect muscle ATP levels may be just as effective as XOR inhibitors.

Targeting UA as an atrophy treatment

XOR inhibitors have been shown to partially attenuate muscle atrophy in conditions of disuse and cancer [54, 67, 69], and high serum UA has shown to be an independent predictor of low muscle mass [115]. In vitro studies have shown high levels of UA to cause oxidative stress in endothelial cells [151, 152], hepatocytes [60], adipocytes [62], and myotubes [70, 117]. In Chapter 3, we show that high UA does not increase protein degradation, markers of oxidative stress, or loss of myotube protein. Thus, these data do not support a direct role for UA in regulating muscle mass. However, UA may still be able to regulate muscle mass indirectly in vivo. For instance, other in vitro studies show high UA treatment can increase production of inflammatory cytokines such IL-6 and IL-1β in endothelial cells [151], macrophages [127, 153], and hepatocytes[63]. These inflammatory cytokines are known to be sufficient to stimulate muscle atrophy if elevated sufficiently [20, 128, 154].

Limitations

A limitation of this study was our inability to determine the quantitative contribution of muscle fiber purines to rises in serum uric acid in vivo. This is challenging to prove

experimentally but is theoretically possible if skeletal muscle specific knockout mice were generated for enzymes of purine nucleotide degradation that allowed inducible but complete abolishment of muscle purine loss. Such approaches would undoubtedly require targeting multiple enzymes simultaneously.

Another potential limitation of this study is that we only examined EDL muscles during our measures of whole muscle purine release. The EDL is anatomically suited for ex vivo incubation because it is thin enough for oxygen to reach its internal fibers, has distinct and accessible tendons needed for anchoring, and can be quickly/easily isolated. However, because it is completely composed of type II fibers [155], our ability to conclude that purine nucleotide degradation is increased during atrophy of muscles with different fiber types is limited. Indeed, differences in the processes we have explored herein likely differ between muscles composed of different fiber types. For example, in mice that were fasted or treated with DEX, AMPD3 protein expression was increased in the TA muscle (composed of a mix of type I, IIa, and IIb fibers) but was unchanged in the EDL muscle (composed primary of type IIb fibers)[155].

Future Directions

Reducing skeletal muscle purine nucleotide degradation and purine release will be necessary to determine its role in muscle atrophy and other tissue pathologies associated with hyperuricemia. We have now demonstrated increased glucocorticoids, FoxO3 activity, and AMPD3 expression are involved in the upregulated purine nucleotide degradation. As such, blocking those events may be accomplished using muscle specific knockout of the glucocorticoid receptor, FoxO's, and AMPD's and a goal for future studies. If these approaches are unable to prevent skeletal muscle purine nucleotide

degradation and purine efflux, then knockout of 5’nucleotidases, which dephosphorylate all purine monophosphates (AMP, GMP, IMP, XMP) and is required for purine release, would be an alternative approach. Additionally, because muscle FoxO activity is inhibited by anabolic hormones such as insulin and IGF-1, determining if the anabolic effects of those hormones require the inhibition of purine nucleotide degradation would be of interest given that anabolic resistance is considered a major contributor to loss of muscle mass.

REFERENCES

[1] Fielding RA, Vellas B, Evans WJ, Bhasin S, Morley JE, Newman AB, et al. Sarcopenia: an undiagnosed condition in older adults. Current consensus definition: prevalence, etiology, and consequences. International working group on sarcopenia. J Am Med Dir Assoc. 2011;12:249-56.

[2] Garnham JO, Roberts LD, Espino-Gonzalez E, Whitehead A, Swoboda PP, Koshy A, et al. Chronic heart failure with diabetes mellitus is characterized by a severe skeletal muscle pathology. Journal of Cachexia, Sarcopenia and Muscle. 2020;11:394-404.

[3] Johansen KL, Shubert T, Doyle J, Soher B, Sakkas GK, Kent-Braun JA. Muscle atrophy in patients receiving hemodialysis: effects on muscle strength, muscle quality, and physical function. Kidney Int. 2003;63:291-7.

[4] Paddon-Jones D, Sheffield-Moore M, Cree MG, Hewlings SJ, Aarsland A, Wolfe RR, et al. Atrophy and impaired muscle protein synthesis during prolonged inactivity and stress. J Clin Endocrinol Metab. 2006;91:4836-41.

[5] Puthucheary ZA, Rawal J, McPhail M, Connolly B, Ratnayake G, Chan P, et al. Acute skeletal muscle wasting in critical illness. JAMA. 2013;310:1591-600.

[6] Levine S, Nguyen T, Taylor N, Friscia ME, Budak MT, Rothenberg P, et al. Rapid disuse atrophy of diaphragm fibers in mechanically ventilated humans. N Engl J Med. 2008;358:1327-35.

[7] Baracos VE, Martin L, Korc M, Guttridge DC, Fearon KCH. Cancer-associated cachexia. Nat Rev Dis Primers. 2018;4:17105.

[8] Iwashyna T, Wesley Ely E, Smith D, Langa K. Long-term cognitive impairment and functional disability among survivors of severe sepsis. JAMA. 2010;304.

[9] Curt G, Breitbart W, Cella D, Groopman J, Horning S, Itri L, et al. Impact of Cancer-Related Fatigue on the Lives of Patients: New Findings From the Fatigue Coalition. The Oncologist. 2000;5:353-60.

[10] Hairi NN, Cumming RG, Naganathan V, Handelsman DJ, Le Couteur DG, Creasey H, et al. Loss of muscle strength, mass (sarcopenia), and quality (specific force) and its relationship with functional limitation and physical disability: the Concord Health and Ageing in Men Project. J Am Geriatr Soc. 2010;58:2055-62.

[11] von Haehling S, Garfias Macedo T, Valentova M, Anker MS, Ebner N, Bekfani T, et al. Muscle wasting as an independent predictor of survival in patients with chronic heart failure. J Cachexia Sarcopenia Muscle. 2020.

[12] Myers J, Prakash M, Froelicher V, Do D, Partington S, Atwood JE. Exercise capacity and mortality among men referred for exercise testing. NEJM. 2002;346.

[13] Rantanen T, Harris T, Leveille S, Visser M, Foley D, Masaki K, et al. Muscle strength and body mass index as long-term predictors of mortality in initially healthy men. Journal of Gerontology. 2000;55.

[14] Zhou X, Wang JL, Lu J, Song Y, Kwak KS, Jiao Q, et al. Reversal of cancer cachexia and muscle wasting by ActRIIB antagonism leads to prolonged survival. Cell. 2010;142:531-43.

[15] Ryan AM, Prado CM, Sullivan ES, Power DG, Daly LE. Effects of weight loss and sarcopenia on response to chemotherapy, quality of life, and survival. Nutrition. 2019;67-68:110539.

[16] Sartori R, Romanello V, Sandri M. Mechanisms of muscle atrophy and hypertrophy: implications in health and disease. Nat Commun. 2021;12:330.

[17] Bodine S, Latres E, Baumhueter S, Lai V, Nunez L, Clarker B, et al. Identification of ubiqutin ligases required for skeletal muscle atrophy. Science. 2001;294.

[18] Sandri M, Sandri C, Gilbert A, Skurk C, Calabria E, Picard A, et al. Foxo transcription factors induce the atrophy-related ubiquitin ligase atrogin-1 and casue skeletal muscle atrophy. Cell. 2004;117:399-412.

[19] Bodine SC, Furlow JD. Glucocorticoids and Skeletal Muscle. Adv Exp Med Biol. 2015;872:145-76.

[20] Bonetto A, Aydogdu T, Jin X, Zhang Z, Zhan R, Puzis L, et al. JAK/STAT3 pathway inhibition blocks skeletal muscle wasting downstream of IL-6 and in experimental cancer cachexia. Am J Physiol Endocrinol Metab. 2012;303:E410-21.

[21] Sartori R, Milan G, Patron M, Mammucari C, Blaauw B, Abraham R, et al. Smad2 and 3 transcription factors control muscle mass in adulthood. Am J Physiol Cell Physiol. 2009;296:C1248-57.

[22] Cai D, Frantz JD, Tawa NE, Jr., Melendez PA, Oh BC, Lidov HG, et al. IKKbeta/NF-kappaB activation causes severe muscle wasting in mice. Cell. 2004;119:285-98.

[23] Stitt T, Drujan D, Clarke B, Panaro F, Timofeyva Y, Kline W, et al. The IGF-1/PI3K/Akt pathway prevents expression of muscle atrophy-induced ubiquitin ligases by inhibiting FOXO transcription factors. Molecular Cell. 2004;14.

[24] Milan G, Romanello V, Pescatore F, Armani A, Paik JH, Frasson L, et al. Regulation of autophagy and the ubiquitin-proteasome system by the FoxO transcriptional network during muscle atrophy. Nat Commun. 2015;6:6670.

[25] Zhao J, Brault JJ, Schild A, Cao P, Sandri M, Schiaffino S, et al. FoxO3 coordinately activates protein degradation by the autophagic/lysosomal and proteasomal pathways in atrophying muscle cells. Cell Metab. 2007;6:472-83.

[26] Wing S, Goldberg A. Glucocorticoids activate the ATP-ubiquitin-dependent proteolytic system in skeletal muscle during fasting. American Journal of Physiology 1993.

[27] May RC, Kelly RA, Mitch WE. Metabolic acidosis stimulates protein degradation in rat muscle by a glucocorticoid-dependent mechanism. J Clin Invest. 1986;77:614-21.

[28] Braun TP, Grossberg AJ, Krasnow SM, Levasseur PR, Szumowski M, Zhu XX, et al. Cancer- and endotoxin-induced cachexia require intact glucocorticoid signaling in skeletal muscle. FASEB J. 2013;27:3572-82.

[29] Li Y, Reid M. NF-κB mediates the protein loss induced by TNF-α in differentiated skeletal muscle myotubes. Am J Physiol Regulatory Integrative Comp Physiol. 2000;279:1165-70.

[30] Lecker SH, Jagoe RT, Gilbert A, Gomes M, Baracos V, Bailey J, et al. Multiple types of skeletal muscle atrophy involve a common program of changes in gene expression. FASEB J. 2004;18:39-51.

[31] Sacheck JM, Hyatt JP, Raffaello A, Jagoe RT, Roy RR, Edgerton VR, et al. Rapid disuse and denervation atrophy involve transcriptional changes similar to those of muscle wasting during systemic diseases. FASEB J. 2007;21:140-55.

[32] Ibebunjo C, Chick JM, Kendall T, Eash JK, Li C, Zhang Y, et al. Genomic and proteomic profiling reveals reduced mitochondrial function and disruption of the neuromuscular junction driving rat sarcopenia. Mol Cell Biol. 2013;33:194-212.

[33] Brocca L, Toniolo L, Reggiani C, Bottinelli R, Sandri M, Pellegrino MA. FoxO-dependent atrogenes vary among catabolic conditions and play a key role in muscle atrophy induced by hindlimb suspension. J Physiol. 2017;595:1143-58.

[34] Mielcarek M, Smolenski RT, Isalan M. Transcriptional Signature of an Altered Purine Metabolism in the Skeletal Muscle of a Huntington's Disease Mouse Model. Front Physiol. 2017;8:127.

[35] Sahlin K, Broberg S. Adenine nucleotide depletion in human muscle during exercise: causality and significance of AMP Deamination. Int J Sports Med. 1990;11.

[36] Hancock CR, Brault JJ, Terjung R. Protecting the cellular energy state during contractions: role of AMP deaminase. Journal of Physiology and Pharmacology. 2006;57.

[37] Hellsten Y, Richter EA, Kiens B, Bangsbo J. AMP deamination and purine exchange in human skeletal muscle during and after intense exercise. Journal of Physiology. 1999;529:909-20.

[38] Miller SG, Hafen PS, Brault JJ. Increased Adenine Nucleotide Degradation in Skeletal Muscle Atrophy. Int J Mol Sci. 2019;21.

[39] Baldwin SA, Beal PR, Yao SY, King AE, Cass CE, Young JD. The equilibrative nucleoside transporter family, SLC29. Pflugers Arch. 2004;447:735-43.

[40] Berry CE, Hare JM. Xanthine oxidoreductase and cardiovascular disease: molecular mechanisms and pathophysiological implications. J Physiol. 2004;555:589-606.

[41] Tsushima Y, Nishizawa H, Tochino Y, Nakatsuji H, Sekimoto R, Nagao H, et al. Uric acid secretion from adipose tissue and its increase in obesity. J Biol Chem. 2013;288:27138-49.

[42] Jarasch ED, Grund C, Bruder G, Held H, Keenan T, Franke W. Localization of xanthine oxidase in mammary-gland epithelium and capillary endothelium. Cell. 1981;25.

[43] Hellsten-Westing Y. Immunohistochemical localization of xanthine oxidase in human cardiac and skeletal muscle. Histochemistry. 1993;100:215-22.

[44] Hellsten-Westing Y, Kaijser L, Ekblom B, Sjodin B. Exchange of purine in human liver and skeletal muscle with short-term exhaustive exercise. American Journal of Physiology. 1993.

[45] Fini M, Elias A, Johnson RJ, Wright R. Contribution of uric acid to cancer risk, recurrence, and mortality. Clinical and Translational Medicine. 2012.

[46] Dehghan A, van Hoek M, Sijbrands EJ, Hofman A, Witteman JC. High serum uric acid as a novel risk factor for type 2 diabetes. Diabetes Care. 2008;31:361-2.

[47] Li L, Yang C, Zhao Y, Zeng X, Liu F, Fu P. Is hyperuricemia an independent risk factor for new-onset chronic kidney disease?: a systemic review and meta-analysis based on observational cohort studies. BMC Nephrology. 2014;15.

[48] Anker SD, Doehner W, Rauchhaus M, Sharma R, Francis D, Knosalla C, et al. Uric acid and survival in chronic heart failure: validation and application in metabolic, functional, and hemodynamic staging. Circulation. 2003;107:1991-7.

[49] Fang J, Alderman M. Serum uric acid and cardiovascular mortality. The NHANES I epidemiologic follow-up study, 1971-1992. JAMA. 2000;283.

[50] Ford ES, Li C, Cook S, Choi HK. Serum concentrations of uric acid and the metabolic syndrome among US children and adolescents. Circulation. 2007;115:2526-32.

[51] Ruggiero C, Cherubini A, Ble A, Bos AJ, Maggio M, Dixit VD, et al. Uric acid and inflammatory markers. Eur Heart J. 2006;27:1174-81.

[52] Cappola TP, Kass DA, Nelson GS, Berger RD, Rosas GO, Kobeissi ZA, et al. Allopurinol improves myocardial efficiency in patients with idiopathic dilated cardiomyopathy. Circulation. 2001;104:2407-11.

[53] George J, Carr E, Davies J, Belch JJ, Struthers A. High-dose allopurinol improves endothelial function by profoundly reducing vascular oxidative stress and not by lowering uric acid. Circulation. 2006;114:2508-16.

[54] Springer J, Tschirner A, Hartman K, Palus S, Wirth EK, Ruis SB, et al. Inhibition of xanthine oxidase reduces wasting and improves outcome in a rat model of cancer cachexia. Int J Cancer. 2012;131:2187-96.

[55] Goicoechea M, de Vinuesa SG, Verdalles U, Ruiz-Caro C, Ampuero J, Rincon A, et al. Effect of allopurinol in chronic kidney disease progression and cardiovascular risk. Clin J Am Soc Nephrol. 2010;5:1388-93.

[56] Nishikawa T, Nagata N, Shimakami T, Shirakura T, Matsui C, Ni Y, et al. Xanthine oxidase inhibition attenuates insulin resistance and diet-induced steatohepatitis in mice. Sci Rep. 2020;10:815.

[57] Chen C, Lu JM, Yao Q. Hyperuricemia-Related Diseases and Xanthine Oxidoreductase (XOR) Inhibitors: An Overview. Med Sci Monit. 2016;22:2501-12.

[58] Yang CY, Chen CH, Deng ST, Huang CS, Lin YJ, Chen YJ, et al. Allopurinol Use and Risk of Fatal Hypersensitivity Reactions: A Nationwide Population-Based Study in Taiwan. JAMA Intern Med. 2015;175:1550-7.

[59] Pacher P, Nivorozhkin A, Szabo C. Therapeutic effects of xanthine oxidase inhibitors: renaissance half a century after the discovery of allopurinol. Pharmacol Rev. 2006;58:87-114.

[60] Lanaspa MA, Sanchez-Lozada LG, Choi YJ, Cicerchi C, Kanbay M, Roncal-Jimenez CA, et al. Uric acid induces hepatic steatosis by generation of mitochondrial oxidative stress: potential role in fructose-dependent and -independent fatty liver. J Biol Chem. 2012;287:40732-44.

[61] Baldwin W, McRae S, Marek G, Wymer D, Pannu V, Baylis C, et al. Hyperuricemia as a mediator of the proinflammatory endocrine imbalance in the adipose tissue in a murine model of the metabolic syndrome. Diabetes. 2011;60:1258-69.

[62] Sautin YY, Nakagawa T, Zharikov S, Johnson RJ. Adverse effects of the classic antioxidant uric acid in adipocytes: NADPH oxidase-mediated oxidative/nitrosative stress. Am J Physiol Cell Physiol. 2007;293:C584-96.

[63] Wan X, Xu C, Lin Y, Lu C, Li D, Sang J, et al. Uric acid regulates hepatic steatosis and insulin resistance through the NLRP3 inflammasome-dependent mechanism. J Hepatol. 2016;64:925-32.

[64] Hong Q, Qi K, Feng Z, Huang Z, Cui S, Wang L, et al. Hyperuricemia induces endothelial dysfunction via mitochondrial Na+/Ca2+ exchanger-mediated mitochondrial calcium overload. Cell Calcium. 2012;51:402-10.

[65] Tani T, Okamoto K, Fujiwara M, Katayama A, Tsuruoka S. Metabolomics analysis elucidates unique influences on purine / pyrimidine metabolism by xanthine oxidoreductase inhibitors in a rat model of renal ischemia-reperfusion injury. Mol Med. 2019;25:40.

[66] Lasley RD, Ely SW, Berne RM, Mentzer RM, Jr. Allopurinol enhanced adenine nucleotide repletion after myocardial ischemia in the isolated rat heart. J Clin Invest. 1988;81:16-20.

[67] Derbre F, Ferrando B, Gomez-Cabrera MC, Sanchis-Gomar F, Martinez-Bello VE, Olaso-Gonzalez G, et al. Inhibition of xanthine oxidase by allopurinol prevents skeletal muscle atrophy: role of p38 MAPKinase and E3 ubiquitin ligases. PLoS One. 2012;7:e46668.

[68] Whidden MA, McClung JM, Falk DJ, Hudson MB, Smuder AJ, Nelson WB, et al. Xanthine oxidase contributes to mechanical ventilation-induced diaphragmatic oxidative stress and contractile dysfunction. J Appl Physiol (1985). 2009;106:385-94.

[69] Ferrando B, Gomez-Cabrera MC, Salvador-Pascual A, Puchades C, Derbre F, Gratas-Delamarche A, et al. Allopurinol partially prevents disuse muscle atrophy in mice and humans. Sci Rep. 2018;8:3549.

[70] Maarman GJ, Andrew BM, Blackhurst DM, Ojuka EO. Melatonin protects against uric acid-induced mitochondrial dysfunction, oxidative stress, and triglyceride accumulation in C2C12 myotubes. J Appl Physiol (1985). 2017;122:1003-10.

[71] Hyatt HW, Powers SK. Mitochondrial Dysfunction Is a Common Denominator Linking Skeletal Muscle Wasting Due to Disease, Aging, and Prolonged Inactivity. Antioxidants (Basel). 2021;10.

[72] Bartziokas K, Papaioannou AI, Loukides S, Papadopoulos A, Haniotou A, Papiris S, et al. Serum uric acid as a predictor of mortality and future exacerbations of COPD. Eur Respir J. 2014;43:43-53.

[73] Xia X, Luo Q, Li B, Lin Z, Yu X, Huang F. Serum uric acid and mortality in chronic kidney disease: A systematic review and meta-analysis. Metabolism. 2016;65:1326-41.

[74] Afzali A, Weiss NS, Boyko EJ, Ioannou GN. Association between serum uric acid level and chronic liver disease in the United States. Hepatology. 2010;52:578-89.

[75] Hellsten Y, Frandsen U, Orthenblad N, Sjodin B, Richter EA. Xanthine oxidase in human skeletal muscle following eccentric exercise: a role in inflammation. Journal of Physiology. 1997;498.

[76] Greiner JV, Glonek T. Intracellular ATP Concentration and Implication for Cellular Evolution. Biology (Basel). 2021;10.

[77] Brosh SB, P.; Zoref-Shani, E.; Sperling, O. De Novo Purine Synthesis in Skeletal Muscle. Biochimica et Biophysica Acta. 1982.

[78] Brocca L, Rossi M, Canepari M, Bottinelli R, Pellegrino MA. Exercise Preconditioning Blunts Early Atrogenes Expression and Atrophy in Gastrocnemius Muscle of Hindlimb Unloaded Mice. Int J Mol Sci. 2021;23.

[79] Okada R, Fujita SI, Suzuki R, Hayashi T, Tsubouchi H, Kato C, et al. Transcriptome analysis of gravitational effects on mouse skeletal muscles under microgravity and artificial 1 g onboard environment. Sci Rep. 2021;11:9168.

[80] Petrany MJ, Swoboda CO, Sun C, Chetal K, Chen X, Weirauch MT, et al. Single-nucleus RNA-seq identifies transcriptional heterogeneity in multinucleated skeletal myofibers. Nat Commun. 2020;11:6374.

[81] Davis PR, Miller SG, Verhoeven NA, Morgan JS, Tulis DA, Witczak CA, et al. Increased AMP deaminase activity decreases ATP content and slows protein degradation in cultured skeletal muscle. Metabolism. 2020;108:154257.

[82] Miller SG, Hafen PS, Law AS, Springer CB, Logsdon DL, O'Connell TM, et al. AMP deamination is sufficient to replicate an atrophy-like metabolic phenotype in skeletal muscle. Metabolism. 2021;123:154864.

[83] Warden SJ, Liu Z, Moe SM. Sex- and Age-Specific Centile Curves and Downloadable Calculator for Clinical Muscle Strength Tests to Identify Probable Sarcopenia. Physical Therapy. 2021;102.

[84] Brault JJ, Pizzimenti NM, Dentel JN, Wiseman RW. Selective inhibition of ATPase activity during contraction alters the activation of p38 MAP kinase isoforms in skeletal muscle. J Cell Biochem. 2013;114:1445-55.

[85] Brault JJ, Jespersen JG, Goldberg AL. Peroxisome proliferator-activated receptor gamma coactivator 1alpha or 1beta overexpression inhibits muscle protein degradation, induction of ubiquitin ligases, and disuse atrophy. J Biol Chem. 2010;285:19460-71.

[86] Bollinger LM, Powell JJ, Houmard JA, Witczak CA, Brault JJ. Skeletal muscle myotubes in severe obesity exhibit altered ubiquitin-proteasome and autophagic/lysosomal proteolytic flux. Obesity (Silver Spring). 2015;23:1185-93.

[87] Bollinger LM, Witczak CA, Houmard JA, Brault JJ. SMAD3 augments FoxO3-induced MuRF-1 promoter activity in a DNA-binding-dependent manner. Am J Physiol Cell Physiol. 2014;307:C278-87.

[88] Wicks K, Hood D. Mitochondrial adaptations in denervated muscle: relationship to muscle performance. American Journal of Physiology Cell Physiology. 1990.

[89] Mitchell WK, Williams J, Atherton P, Larvin M, Lund J, Narici M. Sarcopenia, dynapenia, and the impact of advancing age on human skeletal muscle size and strength; a quantitative review. Front Physiol. 2012;3:260.

[90] Holecek M. Histidine in Health and Disease: Metabolism, Physiological Importance, and Use as a Supplement. Nutrients. 2020;12.

[91] Kochlik B, Gerbracht C, Grune T, Weber D. The Influence of Dietary Habits and Meat Consumption on Plasma 3-Methylhistidine-A Potential Marker for Muscle Protein Turnover. Mol Nutr Food Res. 2018;62:e1701062.

[92] Barclay CJ. Modelling diffusive O(2) supply to isolated preparations of mammalian skeletal and cardiac muscle. J Muscle Res Cell Motil. 2005;26:225-35.

[93] Jensen JB, Moller AB, Just J, Mose M, de Paoli FV, Billeskov TB, et al. Isolation and characterization of muscle stem cells, fibro-adipogenic progenitors, and macrophages from human skeletal muscle biopsies. Am J Physiol Cell Physiol. 2021;321:C257-C68.

[94] McNally JS, Davis ME, Giddens DP, Saha A, Hwang J, Dikalov S, et al. Role of xanthine oxidoreductase and NAD(P)H oxidase in endothelial superoxide production in response to oscillatory shear stress. Am J Physiol Heart Circ Physiol. 2003;285:H2290-7.

[95] Xiang L, Zhang H, Wei J, Tian XY, Luan H, Li S, et al. Metabolomics studies on db/db diabetic mice in skeletal muscle reveal effective clearance of overloaded intermediates by exercise. Anal Chim Acta. 2018;1037:130-9.

[96] Kondo H, Nakagaki I, Sasaki S, Hori S, Itokawa Y. Mechanism of oxidative stress in skeletal muscle atrophied by immobilization. American Journal of Physiology-Endocrinology and Metabolism. 1993.

[97] Ryan MJ, Jackson JR, Hao Y, Leonard SS, Alway SE. Inhibition of xanthine oxidase reduces oxidative stress and improves skeletal muscle function in response to electrically stimulated isometric contractions in aged mice. Free Radic Biol Med. 2011;51:38-52.

[98] Vickers S, Schiller HJ, Hildreth JEK, Bulkley GB. Immunoaffinity localization of the enzyme xanthine oxidase on the outside surface of the endothelial cell plasma membrane. Surgery. 1998;124:551-60.

[99] Idstrom JP, Soussi B, Elander A, Bylund-Fellenius AC. Purine metabolism after in vivo ischemia and reperfusion in rat skeletal muscle. American Journal of Physiology Heart. 1990.

[100] Lindsay TF, Liauw S, Romaschin AD, Walker PM. The effect of ischemia/reperfusion on adenine nucleotide metabolism and xanthine oxidase production in skeletal muscle. J Vasc Surg. 1990;12:8-15.

[101] Dumas JF, Bielicki G, Renou JP, Roussel D, Ducluzeau PH, Malthiery Y, et al. Dexamethasone impairs muscle energetics, studied by (31)P NMR, in rats. Diabetologia. 2005;48:328-35.

[102] Kuo T, Lew MJ, Mayba O, Harris CA, Speed TP, Wang JC. Genome-wide analysis of glucocorticoid receptor-binding sites in myotubes identifies gene networks modulating insulin signaling. Proc Natl Acad Sci U S A. 2012;109:11160-5.

[103] Viguerie N, Picard F, Hul G, Roussel B, Barbe P, Iacovoni JS, et al. Multiple effects of a short-term dexamethasone treatment in human skeletal muscle and adipose tissue. Physiol Genomics. 2012;44:141-51.

[104] Judge SM, Wu CL, Beharry AW, Roberts BM, Ferreira LF, Kandarian SC, et al. Genome-wide identification of FoxO-dependent gene networks in skeletal muscle during C26 cancer cachexia. BMC Cancer. 2014;14:997.

[105] Reed SA, Sandesara PB, Senf SM, Judge AR. Inhibition of FoxO transcriptional activity prevents muscle fiber atrophy during cachexia and induces hypertrophy. FASEB J. 2012;26:987-1000.

[106] Doehner W, Schoene N, Rauchhaus M, Leyva-Leon F, Pavitt DV, Reaveley DA, et al. Effects of xanthine oxidase inhibition with allopurinol on endothelial function and peripheral blood flow in hyperuricemic patients with chronic heart failure: results from 2 placebo-controlled studies. Circulation. 2002;105:2619-24.

[107] Konishi M, Pelgrim L, Tschirner A, Baumgarten A, von Haehling S, Palus S, et al. Febuxostat improves outcome in a rat model of cancer cachexia. J Cachexia Sarcopenia Muscle. 2015;6:174-80.

[108] Khosla UM, Zharikov S, Finch JL, Nakagawa T, Roncal C, Mu W, et al. Hyperuricemia induces endothelial dysfunction. Kidney Int. 2005;67:1739-42.

[109] Kang DH, Park SK, Lee IK, Johnson RJ. Uric acid-induced C-reactive protein expression: implication on cell proliferation and nitric oxide production of human vascular cells. J Am Soc Nephrol. 2005;16:3553-62.

[110] Maharani N, Kuwabara M, Hisatome I. Hyperuricemia and Atrial Fibrillation. Int Heart J. 2016;57:395-9.

[111] Montano-Loza AJ, Meza-Junco J, Prado CM, Lieffers JR, Baracos VE, Bain VG, et al. Muscle wasting is associated with mortality in patients with cirrhosis. Clin Gastroenterol Hepatol. 2012;10:166-73, 73 e1.

[112] Martin L, Birdsell L, Macdonald N, Reiman T, Clandinin MT, McCargar LJ, et al. Cancer cachexia in the age of obesity: skeletal muscle depletion is a powerful prognostic factor, independent of body mass index. J Clin Oncol. 2013;31:1539-47.

[113] Powers SK, Lynch GS, Murphy KT, Reid MB, Zijdewind I. Disease-Induced Skeletal Muscle Atrophy and Fatigue. Med Sci Sports Exerc. 2016;48:2307-19.

[114] Srikanthan P, Karlamangla AS. Relative muscle mass is inversely associated with insulin resistance and prediabetes. Findings from the third National Health and Nutrition Examination Survey. J Clin Endocrinol Metab. 2011;96:2898-903.

[115] Beavers KM, Beavers DP, Serra MC, Bowden RG, Wilson RL. Low releative skeletal muscle mass indicative of sarcopenia is associated with elevations in serum uric acid levels: findings from NHANES III. The Journal of Nutrition, Health and Aging. 2009;13.

[116] Liu X, Chen X, Hu F, Xia X, Hou L, Zhang G, et al. Higher uric acid serum levels are associated with sarcopenia in west China: a cross-sectional study. BMC Geriatr. 2022;22:121.

[117] Yuan H, Hu Y, Zhu Y, Zhang Y, Luo C, Li Z, et al. Metformin ameliorates high uric acid-induced insulin resistance in skeletal muscle cells. Mol Cell Endocrinol. 2017;443:138-45.

[118] Law AS, Hafen PS, Brault JJ. Liquid Chromatography Method for Simultaneous Quantification of ATP and its Degradation Products Compatible with both UV-Vis and Mass Spectrometry. Journal of Chromatography B. 2022.

[119] Cox AG, Winterbourn CC, Hampton MB. Measuring the Redox State of Cellular Peroxiredoxins by Immunoblotting. Thiol Redox Transitions in Cell Signaling, Part B: Cellular Localization and Signaling2010. p. 51-66.

[120] Menconi M, Gonnella P, Petkova V, Lecker S, Hasselgren PO. Dexamethasone and corticosterone induce similar, but not identical, muscle wasting responses in cultured L6 and C2C12 myotubes. J Cell Biochem. 2008;105:353-64.

[121] Sacheck JM, Ohtsuka A, McLary SC, Goldberg AL. IGF-I stimulates muscle growth by suppressing protein breakdown and expression of atrophy-related ubiquitin ligases, atrogin-1 and MuRF1. Am J Physiol Endocrinol Metab. 2004;287:E591-601.

[122] McClung JM, Judge AR, Powers SK, Yan Z. p38 MAPK links oxidative stress to autophagy-related gene expression in cachectic muscle wasting. Am J Physiol Cell Physiol. 2010;298:C542-9.

[123] Ames B, Cathcart R, Schwiers E, Hochstein P. Uric acid provides an antioxidant defense in humans against oxidant- and radical-caused aging and cancer; A hypthesis. PNAS. 1981;78:6858-62.

[124] Peskin AV, Dickerhof N, Poynton RA, Paton LN, Pace PE, Hampton MB, et al. Hyperoxidation of peroxiredoxins 2 and 3: rate constants for the reactions of the sulfenic acid of the peroxidatic cysteine. J Biol Chem. 2013;288:14170-7.

[125] Stretton C, Pugh JN, McDonagh B, McArdle A, Close GL, Jackson MJ. 2-Cys peroxiredoxin oxidation in response to hydrogen peroxide and contractile activity in skeletal muscle: A novel insight into exercise-induced redox signalling? Free Radic Biol Med. 2020;160:199-207.

[126] Dalbeth N, Merriman TR, Stamp LK. Gout. The Lancet. 2016;388:2039-52.

[127] Martinon F, Petrilli V, Mayor A, Tardivel A, Tschopp J. Gout-associated uric acid crystals activate the NALP3 inflammasome. Nature. 2006;440:237-41.

[128] Braun TP, Zhu X, Szumowski M, Scott GD, Grossberg AJ, Levasseur PR, et al. Central nervous system inflammation induces muscle atrophy via activation of the hypothalamic-pituitary-adrenal axis. J Exp Med. 2011;208:2449-63.

[129] Gersch C, Palii SP, Kim KM, Angerhofer A, Johnson RJ, Henderson GN. Inactivation of nitric oxide by uric acid. Nucleosides Nucleotides Nucleic Acids. 2008;27:967-78.

[130] Anderson JE, Zhu A, Mizuno TM. Nitric oxide treatment attenuates muscle atrophy during hind limb suspension in mice. Free Radic Biol Med. 2018;115:458-70.

[131] Yoo JI, Kim MJ, Na JB, Chun YH, Park YJ, Park Y, et al. Relationship between endothelial function and skeletal muscle strength in community dwelling elderly women. J Cachexia Sarcopenia Muscle. 2018;9:1034-41.

[132] Kanellis J, Watanabe S, Li JH, Kang DH, Li P, Nakagawa T, et al. Uric acid stimulates monocyte chemoattractant protein-1 production in vascular smooth muscle cells via mitogen-activated protein kinase and cyclooxygenase-2. Hypertension. 2003;41:1287-93.

[133] Talbert EE, Lewis HL, Farren MR, Ramsey ML, Chakedis JM, Rajasekera P, et al. Circulating monocyte chemoattractant protein-1 (MCP-1) is associated with cachexia in treatment-naive pancreatic cancer patients. J Cachexia Sarcopenia Muscle. 2018;9:358-68.

[134] Wu X, Wakamiya M, Vaishnav S, Geske R, Montgomery C, Jr., Jones P, et al. Hyperuricemia and urate nephropathy in urate oxidase-deficient mice. Proc Natl Acad Sci U S A. 1994;91:742-6.

[135] Lu J, Hou X, Yuan X, Cui L, Liu Z, Li X, et al. Knockout of the urate oxidase gene provides a stable mouse model of hyperuricemia associated with metabolic disorders. Kidney Int. 2018;93:69-80.

[136] Winterbourn CC. Reconciling the chemistry and biology of reactive oxygen species. Nat Chem Biol. 2008;4:278-86.

[137] Murphy MP, Bayir H, Belousov V, Chang CJ, Davies KJA, Davies MJ, et al. Guidelines for measuring reactive oxygen species and oxidative damage in cells and in vivo. Nature Metabolism. 2022;4:651-62.

[138] So A, Thorens B. Uric acid transport and disease. J Clin Invest. 2010;120:1791-9.

[139] Tanaka Y, Nagoshi T, Takahashi H, Oi Y, Yoshii A, Kimura H, et al. URAT1-selective inhibition ameliorates insulin resistance by attenuating diet-induced hepatic steatosis and brown adipose tissue whitening in mice. Mol Metab. 2022;55:101411.

[140] Nie Q, Liu M, Zhang Z, Zhang X, Wang C, Song G. The effects of hyperuricemia on endothelial cells are mediated via GLUT9 and the JAK2/STAT3 pathway. Mol Biol Rep. 2021;48:8023-32.

[141] Spiga R, Marini MA, Mancuso E, Di Fatta C, Fuoco A, Perticone F, et al. Uric Acid Is Associated With Inflammatory Biomarkers and Induces Inflammation Via Activating the NF-kappaB Signaling Pathway in HepG2 Cells. Arterioscler Thromb Vasc Biol. 2017;37:1241-9.

[142] Tullson PC, Terjung RL. Adenine nucleotide degradation in striated muscle. Int J Sports Med. 1990;11 Suppl 2:S47-55.

[143] Meyer RA, Terjung RL. AMP deamination and IMP reamination in working skeletal muscle. Am J Physiol. 1980;239:C32-8.

[144] Braun TP, Marks DL. The regulation of muscle mass by endogenous glucocorticoids. Front Physiol. 2015;6:12.

[145] Felig P. The glucose-alanine cycle. Metabolism. 1973;22:179-207.

[146] He Y, Hakvoort TB, Kohler SE, Vermeulen JL, de Waart DR, de Theije C, et al. Glutamine synthetase in muscle is required for glutamine production during fasting and extrahepatic ammonia detoxification. J Biol Chem. 2010;285:9516-24.

[147] Max S. Glucocorticoid-mediated induction of glutamine synthetase in skeletal muscle. Medicine and Science in Sports and Exercise. 1990;22:325-30.

[148] Fabbrini E, Serafini M, Colic Baric I, Hazen SL, Klein S. Effect of plasma uric acid on antioxidant capacity, oxidative stress, and insulin sensitivity in obese subjects. Diabetes. 2014;63:976-81.

[149] Cohen S, Nathan JA, Goldberg AL. Muscle wasting in disease: molecular mechanisms and promising therapies. Nat Rev Drug Discov. 2015;14:58-74.

[150] Johnson TA, Jinnah HA, Kamatani N. Shortage of Cellular ATP as a Cause of Diseases and Strategies to Enhance ATP. Front Pharmacol. 2019;10:98.

[151] Yang X, Gu J, Lv H, Li H, Cheng Y, Liu Y, et al. Uric acid induced inflammatory responses in endothelial cells via up-regulating(pro)renin receptor. Biomed Pharmacother. 2019;109:1163-70.

[152] Huang Z, Hong Q, Zhang X, Xiao W, Wang L, Cui S, et al. Aldose reductase mediates endothelial cell dysfunction induced by high uric acid concentrations. Cell Commun Signal. 2017;15:3.

[153] Cobo I, Cheng A, Murillo-Saich J, Coras R, Torres A, Abe Y, et al. Monosodium urate crystals regulate a unique JNK-dependent macrophage metabolic and inflammatory response. Cell Rep. 2022;38:110489.

[154] Madaro L, Passafaro M, Sala D, Etxaniz U, Lugarini F, Proietti D, et al. Denervation-activated STAT3-IL-6 signalling in fibro-adipogenic progenitors promotes myofibres atrophy and fibrosis. Nat Cell Biol. 2018;20:917-27.

[155] Bloemberg D, Quadrilatero J. Rapid determination of myosin heavy chain expression in rat, mouse, and human skeletal muscle using multicolor immunofluorescence analysis. PLoS One. 2012;7:e35273.

APPENDIX: APPROVAL LETTERS

ECU

Animal Care and Use Committee
212 Ed Warren Life Sciences Building | East Carolina University | Greenville, NC 27834-4354
252-744-2436 office | 252-744-2355 fax

August 15, 2019

Jeff Brault, Ph.D.
Department of Kinesiology
Brody 3W-40a
East Carolina University

Dear Dr. Brault:

Your Animal Use Protocol entitled, "Impaired Cellular Energetics and Atrophy of Skeletal Muscle" (AUP #P063c) was reviewed by this institution's Animal Care and Use Committee on August 15, 2019. The following action was taken by the Committee:

"Approved as submitted"

Please contact Aaron Hinkle at 744-2997 prior to hazard use

A copy is enclosed for your laboratory files. Please be reminded that all animal procedures must be conducted as described in the approved Animal Use Protocol. Modifications of these procedures cannot be performed without prior approval of the ACUC. The Animal Welfare Act and Public Health Service Guidelines require the ACUC to suspend activities not in accordance with approved procedures and report such activities to the responsible University Official (Vice Chancellor for Health Sciences or Vice Chancellor for Academic Affairs) and appropriate federal Agencies. **Please ensure that all personnel associated with this protocol have access to this approved copy of the AUP and are familiar with its contents.**

Sincerely yours,

SB McRae

Susan McRae, Ph.D.
Chair, Animal Care and Use Committee

SM/jd

Enclosure

The Brody School of Medicine
Office of Prospective Health
East Carolina University
188 Warren Life Sciences Building • Greenville, NC 27834
252-744-2070 office • 252-744-2417 fax

Occupational Medicine
Employee Health
Radiation Safety
Infection Control
Biological Safety

TO: Dr. Jeffrey J. Brault
Department of Kinesiology

FROM: Eddie Johnson
John Baumgartner
Biological Safety Officers

RE: Registration Final Approval

Date: August 9, 2018

Your Biological Safety Protocol, **Impaired Cellular Energetics and Atrophy of Skeletal Muscle** has received **final approval** to be conducted at Biosafety Level 2 and Animal Biosafety Level 1 in Brody 3N-74 and 3W-40 based on your registration/revisions submitted,

using: A. Biohazards

- ☐ Infectious Agent(s)
- ☐ Biotoxin(s)
- ☐ Allergen(s)
- ☐ Prion(s)
- ☒ Human blood, fluid, cells, tissue or cell cultures
- ☐ Transformed cells
- ☐ Other

and/or B. ☒ NIH Use of Recombinant DNA (or RNA) molecules, microorganisms use or breeding transgenic or techniques (plasmids, viral vectors, transfection); of transgenic animals or plants at NIH Category III-D.

This approval is effective for a period of 3 years and may be renewed with an updated registration if needed at that time. Your laboratory will be inspected periodically (every 1-3 years) depending upon the materials/techniques used.

Please notify the Animal Care staff before beginning work with Biohazard agents in animals. Also, please keep in mind all individuals who will be exposed to or handle human-derived biohazardous agents will be due for Blood Borne Pathogens refresher training annually.

Please do not hesitate to contact Biological Safety at 744-2070 if you have any questions, concerns, or need any additional information. Best wishes on your research.

cc: Dr. Daniel Martin, Chair, Biosafety Committee
Dr. Stacey Altman, Department Chair
Janine Davenport, IACUC
Dr. Susan McRae, IACUC
Aaron Hinkle, Comparative Medicine